

1 **Large fresh water influx induced salinity gradient and diagenetic**
2 **changes in the northern Indian Ocean dominate the stable oxygen**
3 **isotopic variation in *Globigerinoides ruber***
4

5 Rajeev Saraswat^{1*}, Thejasino Suokhrie¹, Dinesh K. Naik², Dharmendra P. Singh³, Syed M.
6 Saalim⁴, Mohd Salman^{1,5}, Gavendra Kumar^{1,5}, Sudhira R. Bhadra¹, Mahyar Mohtadi⁶, Sujata R.
7 Kurtarkar¹, Abhayanand S. Maurya³

8 ¹ Micropaleontology Laboratory, National Institute of Oceanography, Goa, India

9 ² Banaras Hindu University, Varanasi, Uttar Pradesh, India

10 ³ Indian Institute of Technology, Roorkee, India

11 ⁴ National Center for Polar and Ocean Research, Goa, India

12 ⁵ School of Earth, Ocean and Atmospheric Sciences, Goa University, Goa

13 ⁶ MARUM, University of Bremen, Bremen, Germany

14 * Correspondence to: Rajeev Saraswat (rsaraswat@nio.org)

15
16 **Abstract.** The application of stable oxygen isotopic ratio of surface dwelling *Globigerinoides ruber* (white variety)
17 ($\delta^{18}\text{O}_{ruber}$) to reconstruct past hydrological changes requires precise understanding of the effect of ambient parameters
18 on $\delta^{18}\text{O}_{ruber}$. The northern Indian Ocean, with huge freshwater influx and being a part of the Indo-Pacific Warm Pool,
19 provides a unique setting to understand the effect of both the salinity and temperature on $\delta^{18}\text{O}_{ruber}$. Here, we use a total
20 of 400 surface samples (252 from this work and 148 from previous studies), covering the entire salinity end member
21 region, to assess the effect of **fresh water influx induced seawater salinity** and temperature on $\delta^{18}\text{O}_{ruber}$ in the northern
22 Indian Ocean. The analyzed surface $\delta^{18}\text{O}_{ruber}$ very well mimics the expected $\delta^{18}\text{O}$ calcite estimated from the modern
23 seawater parameters (temperature, salinity and seawater $\delta^{18}\text{O}$). We report a large diagenetic overprinting of $\delta^{18}\text{O}_{ruber}$
24 in the surface sediments with an increase of 0.18‰ per kilometer increase in water depth. The **fresh water influx**
25 **induced salinity** exerts the major control on $\delta^{18}\text{O}_{ruber}$ ($R^2 = 0.63$) in the northern Indian Ocean, with an increase of
26 0.29‰ per unit increase in salinity. The relationship between temperature and salinity corrected $\delta^{18}\text{O}_{ruber}$ ($\delta^{18}\text{O}_{ruber} -$
27 $\delta^{18}\text{O}_{sw}$) in the northern Indian Ocean [$T = -0.59 * (\delta^{18}\text{O}_{ruber} - \delta^{18}\text{O}_{sw}) + 26.40$] is different than reported previously based
28 on the global compilation of plankton tow $\delta^{18}\text{O}_{ruber}$ data. The revised equations will help in better paleoclimatic
29 reconstruction from the northern Indian Ocean.
30

Formatted: Font color: Custom Color(0,51,204)

Formatted: Font color: Custom Color(0,51,204)

Formatted: Font color: Custom Color(0,51,204)

31 **1. Introduction**

32 The stable oxygen isotopic ratio ($\delta^{18}\text{O}$) of biogenic carbonates is one of the most extensively used marine paleoclimatic
33 proxies (Mulitza et al., 1997; Lea, 2014; Metcalfe et al., 2019; Saraswat et al., 2019). Even though it was initially
34 suggested that the oxygen isotopic fractionation in biogenic carbonates is largely driven by temperature (Urey et al.,
35 1947), subsequent work revealed that besides temperature, salinity and carbonate ion concentration of ambient
36 seawater also affect the biogenic carbonate $\delta^{18}\text{O}$ (Vergnaud-Grazzini, 1976; Spero et al., 1997; Bemis et al., 1998;
37 Spero et al., 1997; Bijma et al., 1999; Mulitza et al., 2003). On longer time-scales, the global ice volume contributes
38 the largest fraction (~1.0-1.2‰) of the glacial-interglacial shift in marine biogenic carbonate $\delta^{18}\text{O}$, at a majority of the
39 locations (Shackleton, 1987; 2000; Lambeck et al., 2014). The ice volume changes induced well-defined shifts in
40 biogenic carbonate $\delta^{18}\text{O}$ during the last several million years. Therefore, the regional evaporation-precipitation, runoff
41 and temperature changes are reconstructed from the global ice-volume corrected biogenic carbonate $\delta^{18}\text{O}$ (Wang et
42 al., 1995; Kallel et al., 1997; Schmidt et al., 2004; Saraswat et al., 2012; 2013; Kessarkar et al., 2013).

43 The $\delta^{18}\text{O}$ of surface dwelling planktic foraminifera *Globigerinoides ruber* ($\delta^{18}\text{O}_{ruber}$) is often used to
44 reconstruct past surface seawater conditions (Saraswat et al., 2012; 2013; Mahesh and Banakar, 2014). ~~The~~
45 ~~relationship between $\delta^{18}\text{O}_{ruber}$ and ambient seawater physico-chemical conditions, however, varies from basin to basin~~
46 ~~(Vergnaud-Grazzini, 1976; Mulitza et al., 2003; Horikawa et al., 2015; Hollstein et al., 2017).~~ Therefore, continuous
47 efforts are made to understand the regional factors affecting $\delta^{18}\text{O}_{ruber}$ (Vergnaud-Grazzini, 1976; Multiza et al., 1997;
48 2003; Waelbroeck et al., 2005; Mohtadi et al., 2011; Horikawa et al., 2015; Hollstein et al., 2017; ; Sanchez et al.,
49 2022). The depth habitat of *G. ruber* in the tropical Atlantic Ocean has been inferred from its stable oxygen isotopic
50 ratio (Farmer et al., 2007). The change in stable oxygen isotopic ratio of planktic foraminifera, including *G. ruber*, is
51 suggested as a proxy to reconstruct upper water column stratification in the tropical Atlantic Ocean, based on the good
52 correlation between $\delta^{18}\text{O}$ and the ambient seawater characteristics (Steph et al., 2009). A few studies suggested a
53 difference in the $\delta^{18}\text{O}$ of various morphotypes of *G. ruber* (sensu stricto and sensu lato) and attributed it to their distinct
54 ecology and depth habitat (L wemark et al., 2005). However, a recent study from the Gulf of Mexico suggested a
55 similar ecology and depth habitat for both the *G. ruber* morphotypes (Thirumalai et al., 2014). The northern Indian
56 Ocean being influenced by huge fresh water influx as well as being a part of the Indo-Pacific Warm Pool (De Deckker,
57 2016), provides a unique setting to understand the effect of large salinity and temperature changes on $\delta^{18}\text{O}_{ruber}$. Earlier,
58 Duplessy et al., (1981) measured $\delta^{18}\text{O}$ of the living *G. ruber* specimens collected from the water column as well as of
59 the dead ones recovered from surface sediments of the northern Indian Ocean. A similar study from the Red Sea and
60 adjoining western Arabian Sea suggested that *G. ruber* calcifies its test in isotopic equilibrium with the ambient
61 seawater, thus tracking the inter-annual subtle change in the salinity and temperature (Kroon and Ganssen, 1989;
62 Ganssen ~~and~~ Kroon, 1991).

63 The temperature influence on $\delta^{18}\text{O}_{ruber}$ is well defined (Multiza et al., 2003). The effect of fresh water influx
64 induced changes in ambient salinity on $\delta^{18}\text{O}_{ruber}$ is, however, debated (D mmer et al., 2020). With the extensive use
65 of $\delta^{18}\text{O}_{ruber}$ to reconstruct regional evaporation-precipitation changes, especially from the monsoon dominated tropical
66 oceans, it is imperative to understand the precise influence of ambient salinity on $\delta^{18}\text{O}_{ruber}$. The ambient seawater pH.

Formatted: Font color: Custom Color(RGB(0,51,204))

Formatted: Font color: Custom Color(RGB(0,51,204))

Formatted: Font color: Custom Color(RGB(0,51,204))

Formatted: Font color: Custom Color(RGB(0,51,204))

Formatted: Font color: Custom Color(RGB(0,51,204))

67 [carbonate ion concentration \(Bijma et al., 1999\)](#), [presence/absence of symbionts \(Jørgensen et al., 1985\)](#) also affect
68 [the isotopic composition of *G. ruber*](#). However, [limited glacial-interglacial variability in these parameters is masked](#)
69 [by the dominance of temperature and fresh water influx induced salinity changes in oxygen isotopic ratio of *G. ruber*](#).

70 Additionally, the diagenetic changes, especially dissolution, also substantially alters the original isotopic composition
71 of the foraminifera shells (Berger and Killingley, 1977; Wu and Berger, 1989; Lohmann, 1995; McCorkle et al., 1997;
72 Wycech et al., 2018). [The dissolution preferentially removes lighter oxygen isotopic ratio rich sections of the shells,](#)
73 [thus increasing the whole shell \$\delta^{18}O_{ruber}\$ \(Berger and Gardner, 1975; Lohmann, 1995; Weinkauff et al., 2020\)](#). To The
74 studies based on the comparison of ambient parameters with the isotopic composition of living specimens collected
75 in plankton tows may not address the complete range of the changes in isotopic signatures during the sinking of the
76 tests from the surface waters post death, and its subsequent deposition in the sediments at the bottom of the sea. As
77 the fossil shells are the sole basis to find out the isotopic ratio of the ambient seawater in the past, the effect of
78 diagenetic changes including the dissolution on foraminifer's oxygen isotopic ratio has to be properly evaluated. Here,
79 we assess the influence of strong salinity gradient, depth induced dissolution and other associated parameters on the
80 stable oxygen isotopic ratio of the surface dwelling planktic foraminifera *G. ruber* (white variety) in the surface
81 sediments of the northern Indian Ocean.

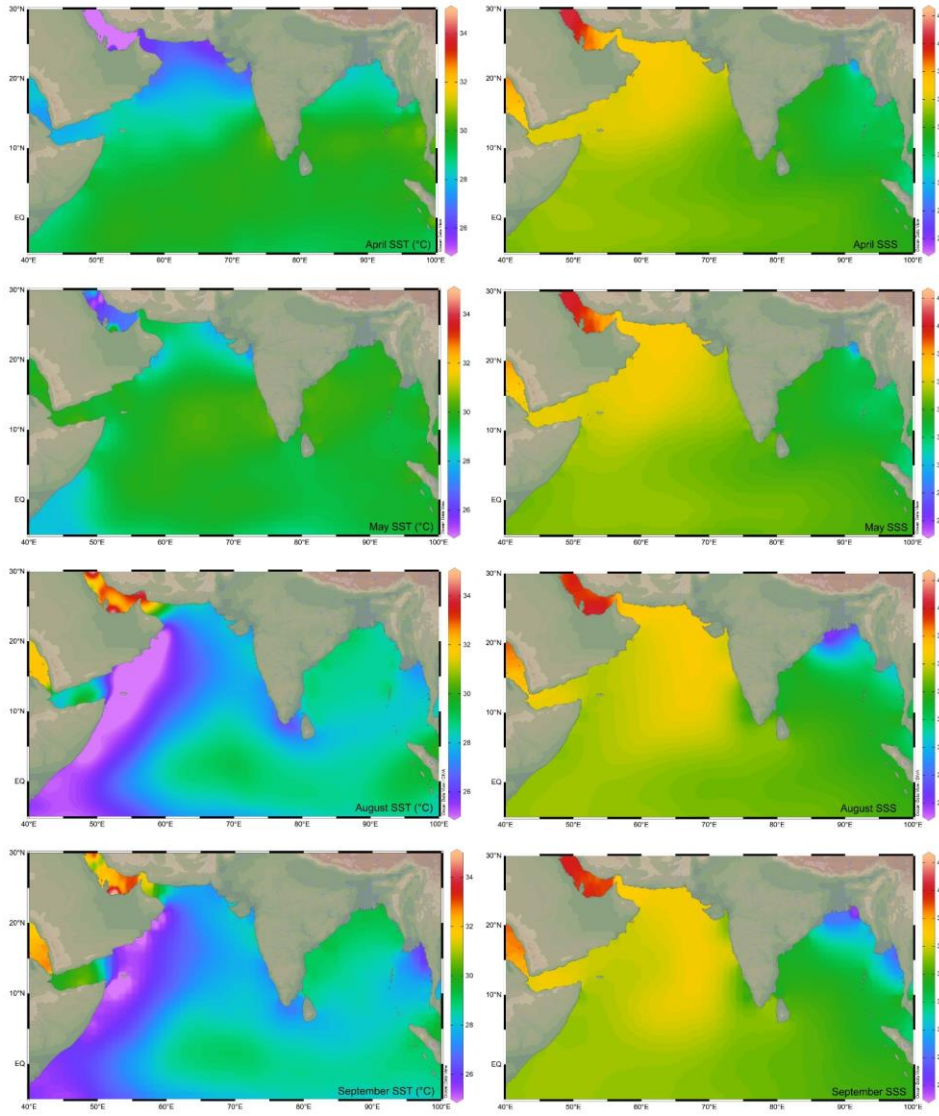
83 2. Ecology of *Globigerinoides ruber* (white)

84 *Globigerinoides ruber* is a spinose planktic foraminifera inhabiting the mixed layer waters, throughout the year, in the
85 tropical-subtropical regions (Guptha et al. 1997; Kemle-von-Mücke and Hemleben 1999). It is one of the dominant
86 planktic foraminifera in the northern Indian Ocean (Bé and Hutson, 1977; Bhadra and Saraswat, 2021) with its relative
87 abundance being as high as ~60% (Fraile et al., 2008). Its test is medium to low trochospiral and hosts algal symbionts
88 (Hemleben et al., 1989). *Globigerinoides ruber* prefers to feed upon phytoplankton (Hemleben et al., 1989), and is
89 dominant in oligotrophic warmer water with optimal temperature being 23.5°C (Fraile et al., 2008). However, it is
90 amongst a few planktic foraminifera species that can tolerate a wide range of salinity (22-49 psu) and temperature
91 (14-31°C) (Hemleben et al., 1989; Guptha et al., 1997). Two varieties of *G. ruber*, namely the white and pink are
92 common in the world oceans. However, the pink variety of *G. ruber* became extinct in the Indian and Pacific Oceans
93 at ~120 kyr during the Marine Isotopic Stage 5e (Thompson et al., 1979).

95 3. Northern Indian Ocean

96 The Indian Ocean with its northern boundary in the tropics includes two hydrographically contrastingly basins, namely
97 the Arabian Sea and Bay of Bengal (BoB) ([Figure 1](#)). The excess of evaporation over precipitation generates high
98 salinity water mass that spreads throughout the surface of the northern Arabian Sea with its core as deep as ~100 m
99 (Shetye et al., 1994; Prasanna Kumar and Prasad, 1999; Joseph and Freeland, 2005). Other high salinity water masses

100 from both the Persian Gulf and Red Sea enter the northern Arabian Sea at deeper depths between 200-400 m and 500-
101 800 m, respectively (Rochford, 1964). A strong upwelling along the western boundary of the Arabian Sea during the
102 summer monsoon season brings cold, nutrient rich subsurface waters to the surface (Chatterjee et al., 2019). The weak
103 upwelling during the same season is also reported in the southeastern Arabian Sea (Smitha et al., 2014).



Formatted: Indent: First line: 0 cm

105 Figure 1: The sea surface temperature (SST) (°C) (Locarnini et al., 2018) and salinity (SSS) (psu) (Zweng et al., 2018) in the
106 northern Indian Ocean during the monsoon (August-September) and non-monsoon (April-May) months. The major rivers
107 draining into the northern Indian Ocean, are marked by blue lines. The map has been prepared by using Ocean Data View
108 software (Schlitzer, 2018).

109
110 The surface water is relatively fresher in the BoB, as the majority of the rivers from the Indian sub-continent drain
111 here, with the total annual continental runoff accounting to 2950 km³ (Sengupta et al., 2006). Additionally, the total
112 annual precipitation over the BoB is 4700 km³, and the evaporation is 3600 km³ (Sengupta et al., 2006). The high
113 salinity Arabian Sea water is transported into the BoB and the fresher BoB water mixes with the high salinity Arabian
114 Sea water, by the seasonally reversing coastal currents (Shankar et al., 2002). The upwelling during summer is
115 restricted to only the northwestern part of the BoB (Shetye et al., 1991). The upwelling combined with the convective
116 mixing during the winter season in the north-eastern Arabian Sea (Madhupratap et al., 1996) as well as eddies in the
117 BoB (Prasanna Kumar et al., 2004; Sarma et al., 2020) result in very high primary productivity in both basins (Qasim,
118 1977; Prasanna Kumar et al., 2009). The high primary productivity and fresh water capping induce strong stratification
119 and restricted circulation that create oxygen deficient zones (ODZ) at the intermediate depth in both the Arabian Sea
120 (Rixen et al., 2020; Naqvi, 2021) and BoB (Bristow et al., 2016, Sridevi and Sarma, 2020). The Arabian Sea ODZ,
121 however, is comparatively thicker and intense, leading to denitrification (Naqvi et al., 2006), which is not reported yet
122 from the BoB (Bristow et al., 2016).

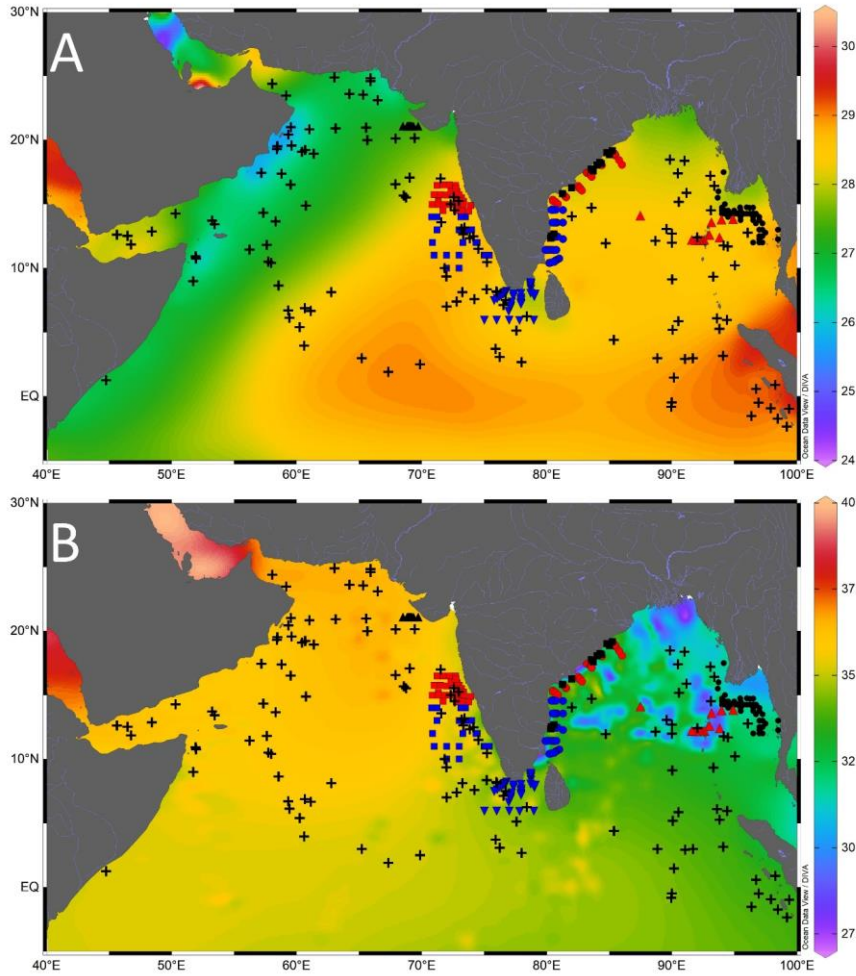
123 The equatorial Indian Ocean forms a part of the Indo-Pacific Warm Pool with sea surface temperature >28
124 °C throughout the year (Vinayachandran and Shetye, 1991; De Deckker, 2016). The marginal regions of the BoB are
125 comparatively warmer due to the fresh water influx from the rivers. The riverine influx shoals the mixed layer and
126 thickens the barrier layer, a buoyant layer separating the thermocline from the pycnocline, in the BoB (Howden and
127 Murtugudde, 2001). The riverine influx flows as a low salinity tongue all along the eastern margin of India (Chaitanya
128 et al., 2014). The annual average sea surface salinity (SSS) is <34 psu throughout the BoB, increasing from the head
129 bay towards south. In contrast to that, SSS remains >35 psu almost throughout the year in the Arabian Sea (Rao and
130 Sivakumar, 2003). The excess of evaporation over precipitation due to the dry northeasterly winds leads to the highest
131 salinity in the northern BoB during the winter (Rao and Sivakumar, 2003).

133 4. Materials and Methodology

134 The surface sediments were collected all along the path of seasonal coastal currents in the northern Indian Ocean
135 (Figure 42, Supplementary Table 1). The samples from the Ayeyarwady Delta Shelf in the northeastern BoB were
136 collected during 'India-Myanmar Joint Oceanographic Studies' onboard Ocean Research Vessel *Sagar Kanya*
137 (SK175). A total of 110 surface sediment samples were collected from the water depths ranging from 10 m to 1080
138 m, on the Ayeyarwady Delta Shelf (Ramaswamy et al., 2008). The multicore samples were also collected at regular
139 intervals in transects running perpendicular to the coast, from the western BoB during the cruise SK308, onboard

Formatted: Font color: Custom Color(RGB(0,51,204))

140 Research Vessel *Sindhu Sadhana* (cruise SSD067) and Research Vessel *Sindhu Sankalp* (cruise SSK35). A total of
141 84 surface samples (including 71 multicore samples and 13 grab samples from sandy sediments) were collected from
142 the inner shelf to outer slope region of the eastern margin of India during the cruise SK308 (Suokhrie et al., 2021 a;
143 Saalim et al., 2022). These samples from the western BoB represent the lowest salinity region in the northern Indian
144 Ocean (Panchang and Nigam, 2012). The multicore samples collected between 25 m and 2980 m in the Gulf of Mannar
145 and the region west of it (43 samples onboard Research Vessel *Sindhu Sadhana* SSD004) represent the zone of cross-
146 basin exchange of seawater between the BoB and the Arabian Sea (Singh et al., 2021). The spade core samples
147 collected from the southeastern Arabian Sea (ORV *Sagar Kanya* cruise SK117 and SK237) are located close to the
148 distal end of the low salinity BoB water intruding into the Arabian Sea. The multicore samples (13 number) collected
149 during SSD055 cruise, from the northeastern Arabian Sea, represent the warm saline conditions. We also collected
150 spade core surface samples from the Andaman Sea, onboard Research Vessel *Sindhu Sankalp* (cruise SSK98). A total
151 of 252 samples had sufficient *G. ruber* for isotopic analysis (Table 1). The new data was augmented with 148
152 previously published core-top studies (e.g. Sirocko, 1989; Prell and Curry, 1981; Duplessy et al., 1981; 1982).
153 Therefore, a total of 400 surface sample data points were used for this study.



154
 155
 156
 157
 158
 159
 160
 161
 162
 163

Figure 12: Location of the core top samples analyzed in this study (black filled triangle - cruise SSD055, red filled square - cruise SK117, blue filled square - cruise SK237, blue filled inverted triangle - cruise SSD004, blue filled circle - cruise SSD067, red filled circle - cruise SK308, black filled square - cruise SSK035, red filled triangle - cruise SSK098, black filled circle - cruise SK175) and the previously published core top values (black plus) compiled from the northern Indian Ocean. The background contours are temperature ($^{\circ}\text{C}$) (A) and salinity (psu) (B) with the scale on the right. Major rivers draining into the northern Indian Ocean, are marked by blue lines. **The map has been prepared by using Ocean Data View software (Schlitzer, 2018).**

Formatted: Font color: Custom Color(RGB(0,51,204))

Table 1: Details of the expedition, number of samples collected in each expedition and the region in which the expedition was held to collect the surface sediment samples used in this study.

Sr.No.	Cruise	Month/Year	Area	Total Samples
1.	SK117	September-October 1996	Eastern Arabian Sea	27
2.	SK175	April-May 2002	North-eastern Bay of Bengal	45
3.	SK237	August 2007	South-eastern Arabian Sea	26
4.	SK308	January 2014	Northwestern Bay of Bengal	29
5.	SSD004	October-November 2014	Gulf of Mannar, Lakshadweep Sea	41
6.	SSD055	August 2018	North-eastern Arabian Sea	11
7.	SSD067	November-December 2019	South-western Bay of Bengal, Lakshadweep Sea, Eastern Arabian Sea	45
8.	SSK035	May-June 2012	Western Bay of Bengal	13
9.	SSK098	January-February 2017	Andaman Sea	15

The surface sediment samples (0-1 cm) were processed following the standard procedure (Suokhrie et al., 2021 b). The freeze-dried sediments were weighed and wet sieved by using 63 μm sieve. The coarse fraction ($>63 \mu\text{m}$) was dry sieved by using 250 μm and 355 μm sieves. For $\delta^{18}\text{O}$ analysis, 10-15 well preserved shells of *G. ruber* white variety were picked from 250-355 μm size range. We picked *G. ruber* s.s. wherever sufficient specimens were available. Unfortunately, several samples yielded very small carbonate fraction. In such samples, we picked mixed population of *G. ruber* to get sufficient specimens for isotopic analysis. The $\delta^{18}\text{O}_{ruber}$ was measured by using Finnigan MAT 253 isotope ratio mass spectrometer, coupled with Kiel IV automated carbonate preparation device. The samples were analyzed in the Alfred Wegner Institute for Polar and Marine Research, Bremerhaven, MARUM, University of Bremen, Bremen, Germany and the Stable Isotope Laboratory (SIL) at Indian Institute of Technology, Roorkee, India. The reference material NBS 18 limestone was used as the calibration material and a secondary in-house standard was run after every 5 samples to detect and correct the drift. The precision of oxygen isotope measurements was better than 0.08‰. The $\delta^{18}\text{O}_{ruber}$ data generated on the newly collected surface sediments was augmented with the published core-top $\delta^{18}\text{O}$ measurements in the northern Indian Ocean. A total of 400 surface sediment data points (252 from this work and 148 from the previous studies) were used to understand the factors affecting $\delta^{18}\text{O}_{ruber}$ in the northern Indian Ocean (Supplementary Table 1). The annual average sea surface temperature and salinity of the top 30 m water column at the respective sample locations was downloaded from the World Ocean Atlas (Boyer et al., 2013). The salinity and temperature at the core location was extrapolated from the nearby grid points, using the Live Access Server at the National Institute of Oceanography, Goa, India.

The analyzed $\delta^{18}\text{O}_{ruber}$ data was compared with the expected $\delta^{18}\text{O}$ calcite to ascertain whether the *G. ruber* properly represents the ambient conditions. For the expected $\delta^{18}\text{O}$ calcite, the $\delta^{18}\text{O}_{sw}$ was calculated from the ambient salinity by using the regional seawater salinity and its stable oxygen isotopic ($\delta^{18}\text{O}_{sw}$) ratio for the entire northern

Formatted Table

Formatted: Font: Not Bold

Formatted: Font: Not Bold

Formatted: Font: Not Bold

Formatted: Font: Not Bold

Formatted: Font: Not Bold

Formatted: List Paragraph, Numbered + Level: 1 + Numbering Style: 1, 2, 3, ... + Start at: 1 + Alignment: Left + Aligned at: 0 cm + Indent at: 0.63 cm

Formatted: Centered

Formatted: Centered

Formatted: Font: (Default) Times New Roman, 9 pt

Formatted

Formatted: Centered

Formatted: Centered

Formatted: Font: Not Bold

Formatted: Font: Not Bold

Formatted: Font: Not Bold

Formatted: Font: Not Bold

Formatted: Centered

Formatted: Font: Not Bold

Formatted

Formatted: Centered

Formatted: Font: Not Bold

Formatted

Formatted: Font: Not Bold

Formatted: Font: Not Bold

Formatted: Centered

Formatted: Font: Not Bold

Formatted: Font: Not Bold

Formatted: Centered

Formatted: Font: Not Bold

Formatted: Font: (Default) Times New Roman, 9 pt

Formatted

Formatted: Centered

Formatted: Font: (Default) Times New Roman, 9 pt

Formatted

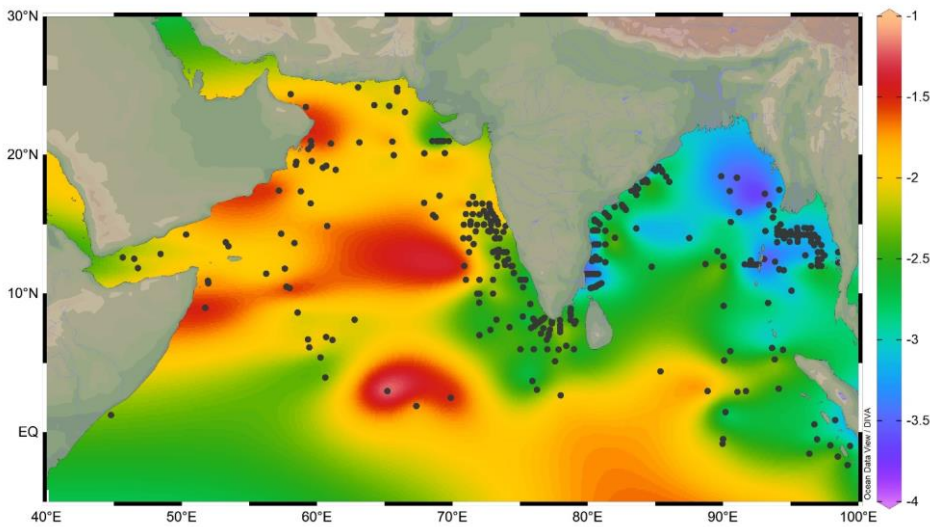
Formatted: Centered

Formatted: Font color: Custom Color(RGB(0,51,204))

188 Indian Ocean (5°S to 30°N). The seawater salinity and corresponding $\delta^{18}\text{O}_{\text{sw}}$ data was downloaded from the Schmidt
189 et al., (1999) (version 1.22) and augmented with other regional datasets (Delaygue et al., 2001; Singh et al., 2010;
190 Achyuthan et al., 2013).
191

192 5. Results

193 The oxygen isotopic ratio of *G. ruber* varies from a minimum of -3.82‰ to the maximum of -1.09‰ in the surface
194 sediments of the northern Indian Ocean (Figure 23). The most depleted $\delta^{18}\text{O}_{\text{ruber}}$ was in the eastern BoB and the most
195 enriched values were in the western Arabian Sea.



196
197
198 **Figure 23:** The variation in *Globigerinoides ruber* $\delta^{18}\text{O}$ (‰) in the surface sediments of the northern Indian Ocean. The
199 stations are marked by black filled circle. The lowest $\delta^{18}\text{O}_{\text{ruber}}$ is in the riverine influx influenced northern Bay of Bengal
200 and the highest is in the evaporation dominated central and western Arabian Sea. The major rivers are marked with thin
201 blue lines. The map has been prepared by using Ocean Data View software (Schlitzer, 2018).
202

203 The east-west gradient in $\delta^{18}\text{O}_{\text{ruber}}$ was also evident in its significant correlation ($R^2 = 0.5$, $n = 400$) with the longitude
204 (Figure 3A4A). However, $\delta^{18}\text{O}_{\text{ruber}}$ did not have any systematic latitudinal variation (Figure 3B4B).

Formatted: Font color: Custom Color(RGB(0,51,204))

Formatted: Font color: Custom Color(RGB(0,51,204))

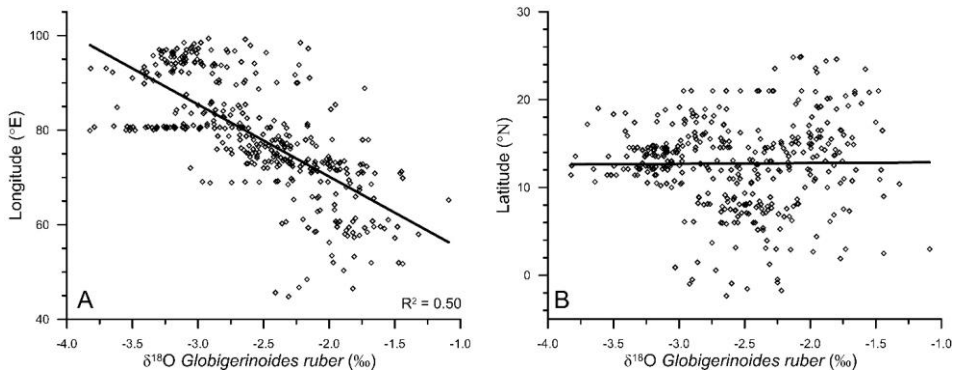
Formatted: Font color: Custom Color(RGB(0,51,204))

Formatted: Font color: Custom Color(RGB(0,51,204)),
Superscript

Formatted: Font color: Custom Color(RGB(0,51,204))

Formatted: Font color: Custom Color(RGB(0,51,204))

Formatted: Font color: Custom Color(RGB(0,51,204))

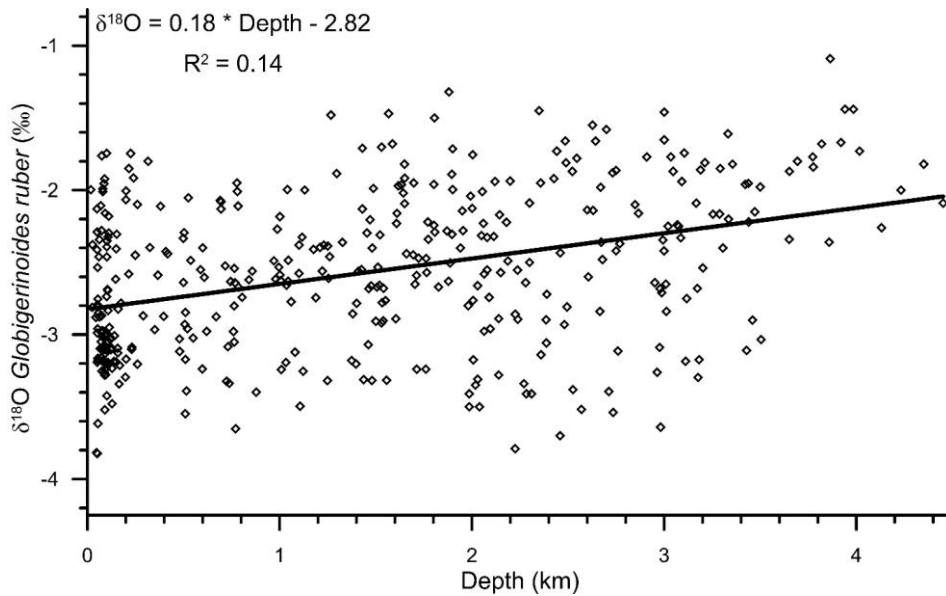


205
206
207 **Figure 34:** The variation in *Globigerinoides ruber* $\delta^{18}\text{O}$ (‰) with the corresponding longitude (A) and latitude (B), in the
208 surface sediments of the northern Indian Ocean.

Formatted: Font color: Custom Color(RGB(0,51,204))

209
210 A significant correlation ($R^2 = 0.14$, $n = 400$) was observed between the water depth and $\delta^{18}\text{O}_{\text{ruber}}$ (Figure 45). $\delta^{18}\text{O}_{\text{ruber}}$
211 increased with increasing depth. The increase was gradual, without any abrupt change.

Formatted: Font color: Custom Color(RGB(0,51,204))



212
213
214 **Figure 45:** The relationship between water depth and the oxygen isotopic ratio of mixed layer dwelling *Globigerinoides*
215 *ruber*. The trendline signifies the relative enrichment of $\delta^{18}\text{O}_{\text{ruber}}$ shells in surface sediments, with increasing water depth.
216

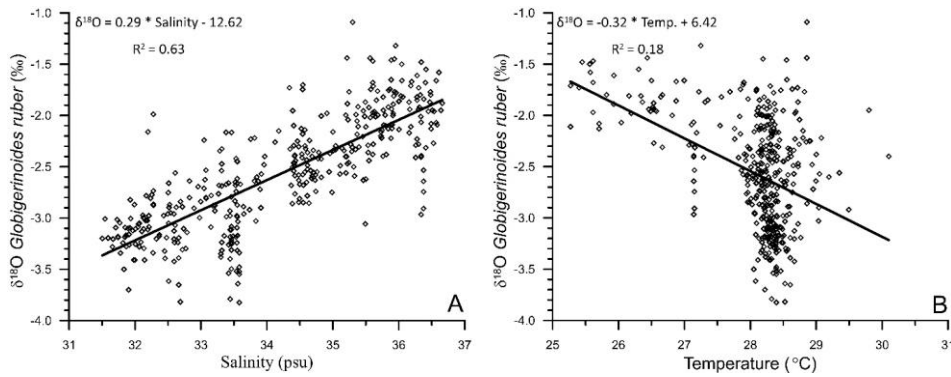
Formatted: Font color: Custom Color(RGB(0,51,204))

217
218
219
220
221
222

The uncorrected $\delta^{18}\text{O}_{ruber}$ was significantly correlated ($R^2 = 0.63$, $n = 400$) with the ambient salinity (Figure 5A6A). However, the relationship between uncorrected $\delta^{18}\text{O}_{ruber}$ and ambient temperature was not as robust ($R^2 = 0.18$, $n = 400$) (Figure 5B6B). A large scatter ($\sim -3.8\text{‰}$ to -1.4‰) was observed in the $\delta^{18}\text{O}_{ruber}$ of the samples collected from a narrow range of ambient temperature (28-29°C) (Figure 6B).

Formatted: Font color: Custom Color(RGB(0,51,204))

Formatted: Font color: Custom Color(RGB(0,51,204))



223
224
225
226
227

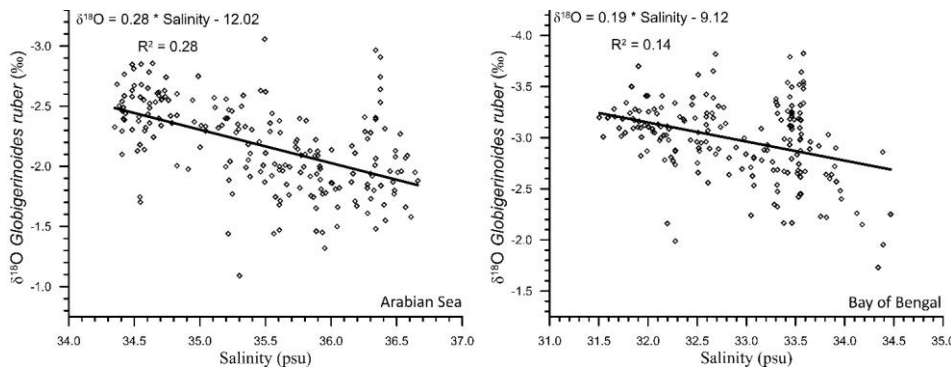
Figure 56: The relationship between stable oxygen isotopic ratio of mixed layer dwelling *Globigerinoides ruber* and annual average mixed layer salinity (A) and temperature (B) in the northern Indian Ocean.

Formatted: Font color: Custom Color(RGB(0,51,204))

228

As the northern Indian Ocean includes two contrasting basins, $\delta^{18}\text{O}_{ruber}$ -salinity relationship was explored for both the Arabian Sea and the BoB. A significant $\delta^{18}\text{O}_{ruber}$ -salinity relationship was observed for both the Arabian Sea ($R^2 = 0.28$, $n = 205$) and BoB ($R^2 = 0.14$, $n = 195$) (Figure 67). We report a different $\delta^{18}\text{O}_{ruber}$ -salinity relationship in these two basins. $\delta^{18}\text{O}_{ruber}$ increased with increasing salinity in both the BoB and the Arabian Sea.

Formatted: Font color: Custom Color(RGB(0,51,204))



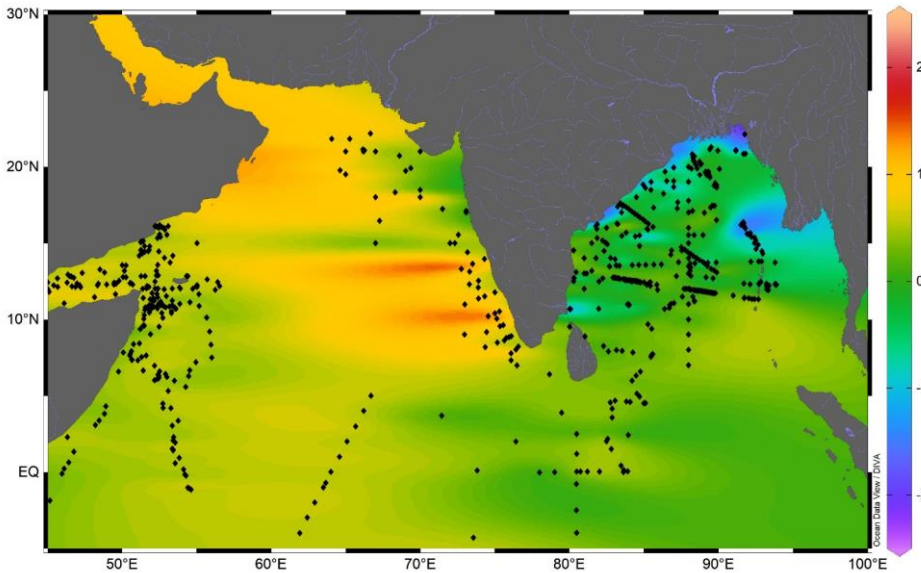
233

234
235
236 **Figure 67:** The relationship between the stable oxygen isotopic ratio of mixed layer dwelling *Globigerinoides ruber* and
237 annual average mixed layer salinity in the Arabian Sea and Bay of Bengal.

Formatted: Font color: Custom Color(RGB(0,51,204))

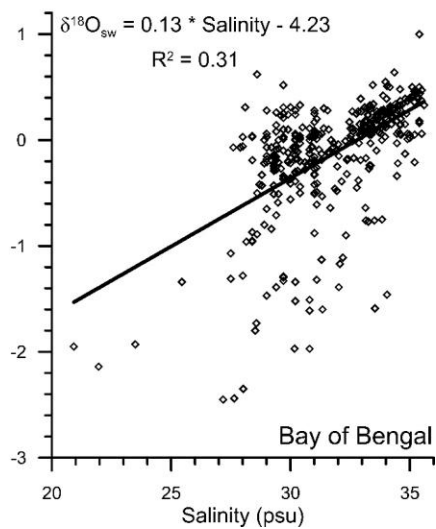
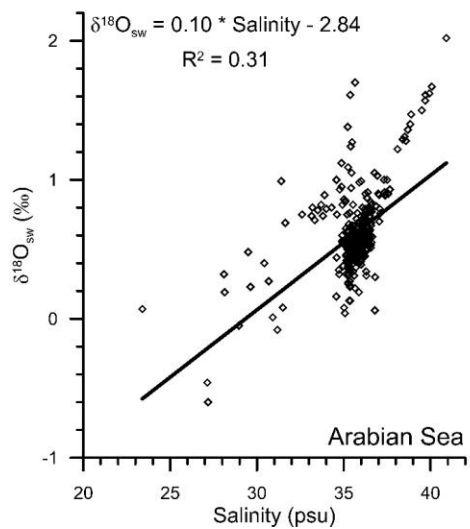
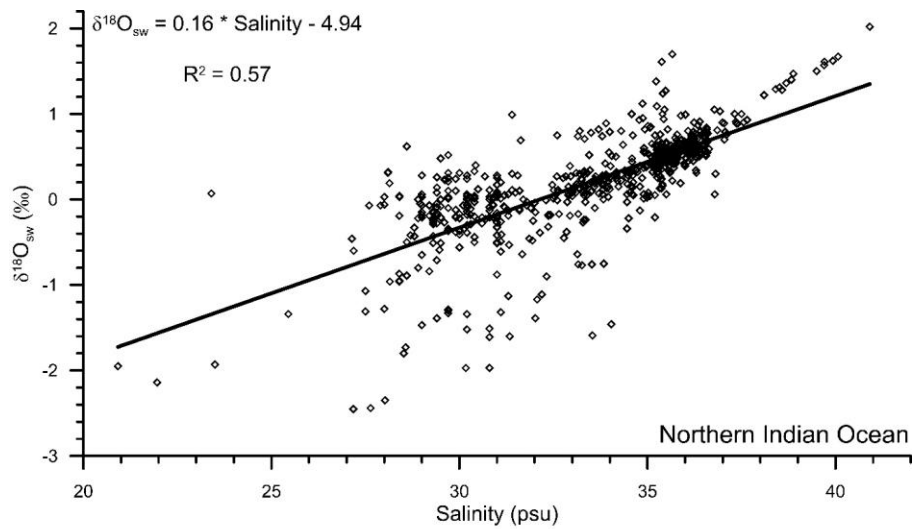
238
239 The dataset to derive the regional salinity- $\delta^{18}\text{O}_{\text{sw}}$ relationship comprises of a total of 750 stations with salinity varying
240 from 20.92 psu to 40.91 psu. The dataset also covered a large range of $\delta^{18}\text{O}_{\text{sw}}$, varying from a minimum of -2.45‰ to
241 the maximum of 2.02‰ (Figure 78, 89). The measured $\delta^{18}\text{O}_{\text{ruber}}$ is strongly correlated ($R^2 = 0.56$, $n = 400$) with the
242 expected $\delta^{18}\text{O}_{\text{calcite}}$, as estimated by using the salinity- $\delta^{18}\text{O}_{\text{sw}}$ relationship and the ambient temperature. However, the
243 relationship between seawater temperature and $\delta^{18}\text{O}_{\text{ruber}}-\delta^{18}\text{O}_{\text{sw}}$, was not very robust. It should however, be noted here
244 that the stratigraphic information is not provided for most of the core tops. Core top sediments can represent older
245 time slices when the sedimentation rates are low or when older sediments are exposed due to erosional processes. This
246 does not matter so much if the Holocene is present and stable. However, in the Indian Ocean, large Holocene $\delta^{18}\text{O}$
247 variations are expected due to variations in monsoon precipitation. Therefore, the uncertain age of the core tops can
248 affect the results stated above.

Formatted: Font color: Custom Color(RGB(0,51,204))



249
250
251 **Figure 78:** The surface seawater oxygen isotopic ratio (‰) in the northern Indian Ocean. The black filled circles are the
252 seawater sample locations compiled from previous studies. The thin blue lines are the major rivers draining in the northern
253 Indian Ocean. The map has been prepared by using Ocean Data View software (Schlitzer, 2018).
254

Formatted: Font color: Custom Color(RGB(0,51,204))



255
256
257

258 **Figure 89:** The relationship between surface water oxygen isotopic ratio and salinity in the northern Indian Ocean (5°S-
259 30°N), Arabian Sea and the Bay of Bengal. The data points are from Schmidt et al., (1999), Delaygue et al., (2001), Singh et
260 al., (2010), and Achyuthan et al., (2013).

261

Formatted: Font color: Custom Color(RGB(0,51,204))

262 **6. Discussion**

263 **6.1 Expected versus analyzed $\delta^{18}\text{O}$**

264 The estimation of expected $\delta^{18}\text{O}$ carbonate requires known seawater $\delta^{18}\text{O}$ values. The seawater $\delta^{18}\text{O}$, however, was
265 not measured. Therefore, the salinity- $\delta^{18}\text{O}_{\text{sw}}$ relationship established from the previous regional seawater isotope and
266 salinity measurements was used. The salinity- $\delta^{18}\text{O}_{\text{sw}}$ relationship varies seasonally as well as from region to region
267 (Singh et al., 2010; Achyuthan et al., 2013; Tiwari et al., 2013). Therefore, it was difficult to choose the appropriate
268 salinity- $\delta^{18}\text{O}_{\text{sw}}$ relationship. Initially, all the data points were clubbed to establish the salinity- $\delta^{18}\text{O}_{\text{sw}}$ relationship. By
269 comparing the measured $\delta^{18}\text{O}_{\text{sw}}$ with the ambient salinity, we established the following relationship for the entire
270 northern Indian Ocean (north of 5°S latitude) ($R^2 = 0.57$, $n = 750$) (Figure 89).

271
272
$$\delta^{18}\text{O}_{\text{sw}} = 0.16 * \text{Salinity} - 4.94 \quad \text{Northern Indian Ocean } (R^2 = 0.57)$$

273
274 Previously, a large difference in the slope of salinity- $\delta^{18}\text{O}_{\text{sw}}$ equation has been reported from the Arabian Sea and the
275 BoB (Delaygue et al., 2001; Singh et al., 2010; Achyuthan et al., 2013). Therefore, we also plotted the salinity- $\delta^{18}\text{O}_{\text{sw}}$
276 separately for the Arabian Sea and BoB (Figure 89). The salinity- $\delta^{18}\text{O}_{\text{sw}}$ relationship for these two basins was
277 represented by the following equations.

278
279
$$\delta^{18}\text{O}_{\text{sw}} = 0.10 * \text{Salinity} - 2.84 \quad \text{Arabian Sea} \quad (R^2 = 0.31, n = 375)$$

280
281
$$\delta^{18}\text{O}_{\text{sw}} = 0.13 * \text{Salinity} - 4.23 \quad \text{Bay of Bengal} \quad (R^2 = 0.31, n = 375)$$

282
283 The continuous flux of *G. ruber* throughout the year (Guptha et al., 1997) and the accumulation of shells in the
284 sediments over a large interval, implies that the salinity- $\delta^{18}\text{O}_{\text{sw}}$ relationship based on data representing all seasons will
285 provide a better estimate of the average $\delta^{18}\text{O}_{\text{ruber}}$ as recovered from the sediments (Vergnaud-Grazzini, 1976). The
286 expected $\delta^{18}\text{O}_{\text{sw}}$ was calculated by using these equations and the annual average mixed layer salinity at the stations
287 for which $\delta^{18}\text{O}_{\text{ruber}}$ data were available. The mixed layer was defined as the top 25 m of the water column following
288 Narvekar and Prasanna Kumar (2014). Although the mixed layer depth varies regionally as well as during different
289 seasons, the average mixed layer depth was used to compare the calcification conditions. A correction factor of 0.27%
290 was applied to convert $\delta^{18}\text{O}_{\text{sw}}$ from SMOW to PDB scale (Hut, 1987). The expected $\delta^{18}\text{O}$ calcite was then estimated
291 from the calculated $\delta^{18}\text{O}_{\text{sw}}$ and the annual average mixed layer temperature by using the equation proposed by Mulitza
292 et al., (2003). We also estimated the expected $\delta^{18}\text{O}$ calcite by using the low-high-light equation of Bemis et al (1998),
293 as *G. ruber* $\delta^{18}\text{O}$ is better described with the high-light equation (Thunell et al. 1999). The choice of equation used to
294 estimate the expected $\delta^{18}\text{O}$ calcite did not make any difference other than a small constant offset. The difference
295 between expected $\delta^{18}\text{O}$ calcite estimated using paleotemperature equation of Mulitza et al., (2003) and the high-light
296 equation of Bemis et al., (1998) varied from -0.33 to -0.41‰. The expected $\delta^{18}\text{O}$ calcite estimated using Mulitza et
297 al., (2003) paleotemperature equation provided values close to the measured *G. ruber* $\delta^{18}\text{O}$. From the scatter plot

Formatted: Font color: Custom Color(RGB(0,51,204))

Formatted: Font color: Custom Color(RGB(0,51,204))

Formatted: Font: Italic, Font color: Custom Color(RGB(0,51,204))

Formatted: Font color: Custom Color(RGB(0,51,204))

Formatted: Font color: Custom Color(RGB(0,51,204)), Superscript

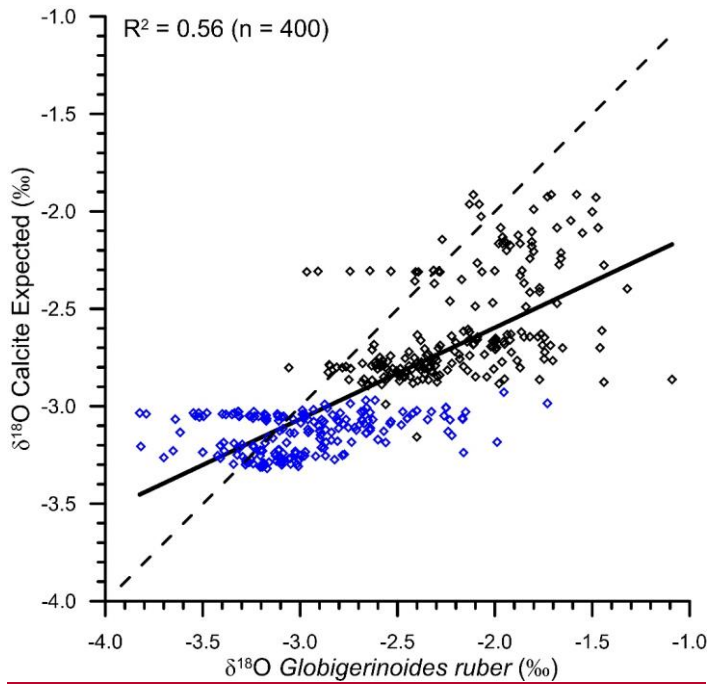
Formatted: Font color: Custom Color(RGB(0,51,204))

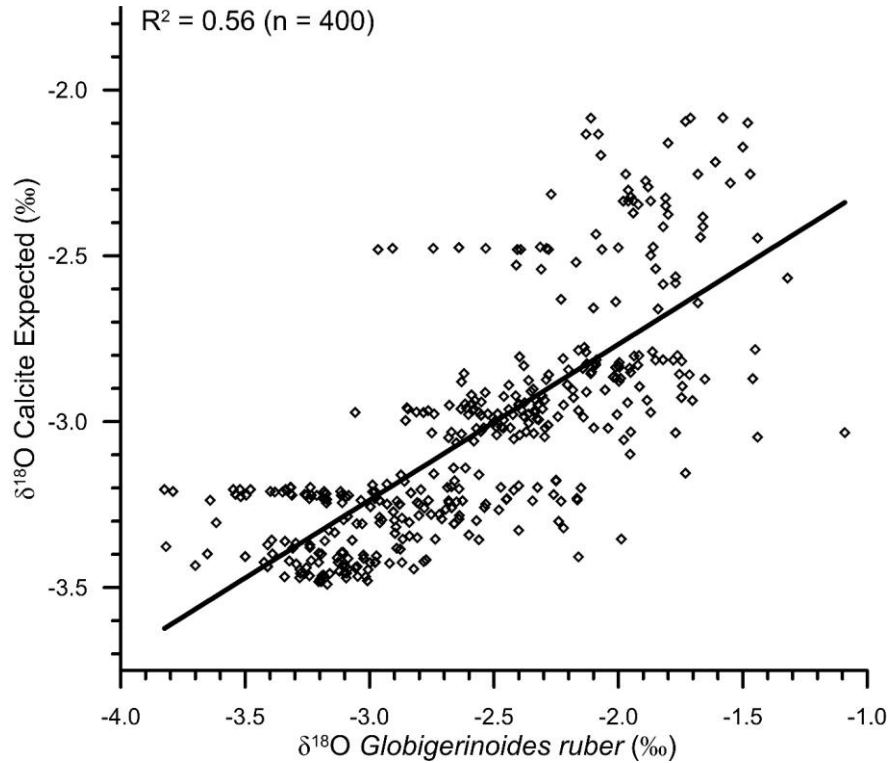
Formatted: Font color: Custom Color(RGB(0,51,204))

Formatted: Font color: Custom Color(RGB(0,51,204))

298 (Figure 910), it was clear that the analyzed $\delta^{18}\text{O}_{ruber}$ was significantly correlated ($R^2 = 0.56$, $n = 400$) with the expected
299 $\delta^{18}\text{O}$ calcite, suggesting that *G. ruber* correctly represents the ambient conditions in the entire northern Indian Ocean.
300 The expected $\delta^{18}\text{O}$ calcite estimated by using the separate Arabian Sea and BoB salinity- $\delta^{18}\text{O}_{sw}$ equations, was also
301 similarly correlated with the analyzed $\delta^{18}\text{O}_{ruber}$.

Formatted: Font color: Custom Color(RGB(0,51,204))



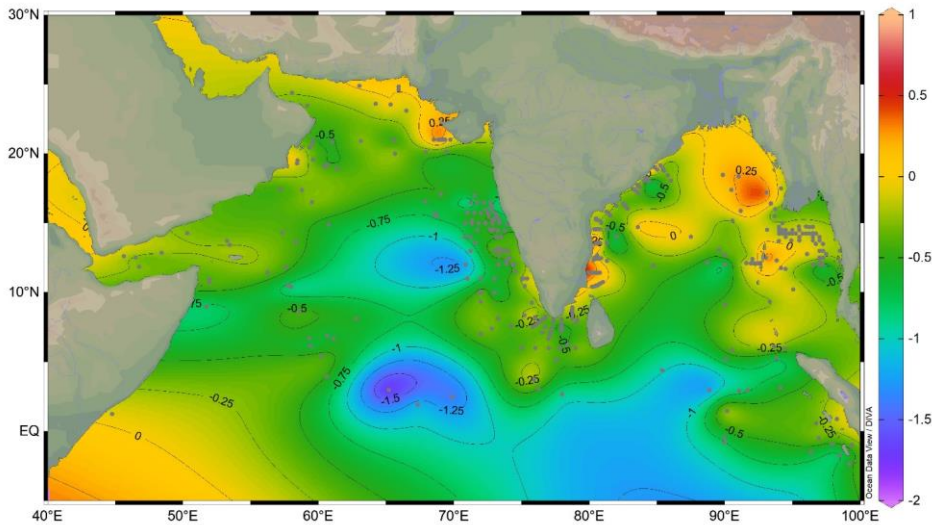


303
304
305 **Figure 910:** The scatter plot of expected $\delta^{18}\text{O}$ calcite (as estimated from the ambient salinity-temperature) and the analyzed
306 $\delta^{18}\text{O}_{\text{ruber}}$. The two are significantly correlated ($R^2 = 0.6356$), suggesting that *Globigerinoides ruber* correctly represents the
307 ambient conditions. **The blue diamonds are the samples collected from the Bay of Bengal and the black diamonds represent**
308 **the samples collected from the Arabian Sea. The dotted line represents the 1:1 relationship between the measured and**
309 **expected $\delta^{18}\text{O}$.**

Formatted: Font color: Custom Color(RGB(0,51,204))

310
311 The deviation of the expected $\delta^{18}\text{O}_{\text{calcite}}$ from the observed $\delta^{18}\text{O}_{\text{ruber}}$ ($\delta^{18}\text{O}_{\text{residual}}$) can be because of several factors
312 including the difference in the ambient conditions at the time of secretion of the primary calcite during the lifetime
313 and the diagenetic changes post death and burial. The observed $\delta^{18}\text{O}_{\text{ruber}}$ was close to the expected $\delta^{18}\text{O}_{\text{calcite}}$ in the
314 shallower waters, especially the BoB, Andaman Sea and northeastern Arabian Sea (Figure 11). The difference was
315 large in the deeper Arabian Sea and the equatorial Indian Ocean. *Globigerinoides ruber* is suggested to inhabit
316 chlorophyll maximum for easy availability of food (Fairbanks and Weibe, 1980). In such a scenario, $\delta^{18}\text{O}_{\text{ruber}}$ is
317 expected to be higher due to lower temperatures and lower light levels at relatively deeper depths (Spero et al., 1997).
318 The depth of chlorophyll maximum is shallower in the marginal marine waters of both the BoB and the Arabian Sea
319 (Sarma & Aswanikumar, 1991; Madhu et al., 2006). If *G. ruber* thrived at chlorophyll maximum depths, the $\delta^{18}\text{O}_{\text{ruber}}$
320 should be enriched in heavier isotope and thus $\delta^{18}\text{O}_{\text{residual}}$ should be negative. The positive $\delta^{18}\text{O}_{\text{residual}}$ in the shallower

321 regions, however, suggests that *G. ruber* thrives in the warmer upper parts of the mixed layer. Alternatively, the large
 322 influence of the depleted fresh water $\delta^{18}\text{O}$ dominates the chlorophyll maximum influence on the observed $\delta^{18}\text{O}_{ruber}$ in
 323 the shallower regions of the northern Indian Ocean. The concentration of positive $\delta^{18}\text{O}_{residual}$ values close to the riverine
 324 influx regions confirms the strong influence of depleted fresh water $\delta^{18}\text{O}$ in modulating $\delta^{18}\text{O}_{ruber}$ in the northern Indian
 325 Ocean. The negative $\delta^{18}\text{O}_{residual}$ at deeper stations is attributed to a combination of factors including deeper chlorophyll
 326 maximum depth habitat of *G. ruber*, reduced influence of fresh water, lower sedimentation rate resulting in mixing of
 327 older and younger fauna, and post depositional diagenetic changes.



328
 329 Figure 11: The difference in the expected $\delta^{18}\text{O}_{calcite}$ and observed $\delta^{18}\text{O}_{ruber}$ in the surface sediments of the northern Indian
 330 Ocean. The grey filled squares are the sample locations. The thin blue lines are the major rivers draining in the northern
 331 Indian Ocean. The thin black lines mark the contours at 0.25‰ interval. The map has been prepared by using Ocean Data
 332 View software (Schlitzer, 2018).
 333

334 **6.2 Latitudinal and Longitudinal variation in $\delta^{18}\text{O}_{ruber}$**

335 We report a strong ($R^2 = 0.50$) longitudinal influence on $\delta^{18}\text{O}_{ruber}$. A similar relationship with the latitudes is missing.
 336 The strong longitudinal signature in $\delta^{18}\text{O}_{ruber}$ is attributed to the large salinity gradient. The huge fresh water influx in
 337 the BoB reduces the SSS in the eastern Indian Ocean. The lack of major rivers in the western Arabian Sea results in
 338 strong low to high salinity gradient from east to west. Although the equatorial and nearby regions are a part of the
 339 Indo-Pacific Warm Pool, the limited temperature variability is evident in the insignificant latitudinal influence on
 340 $\delta^{18}\text{O}_{ruber}$.
 341

342 6.3 Diagenetic alteration

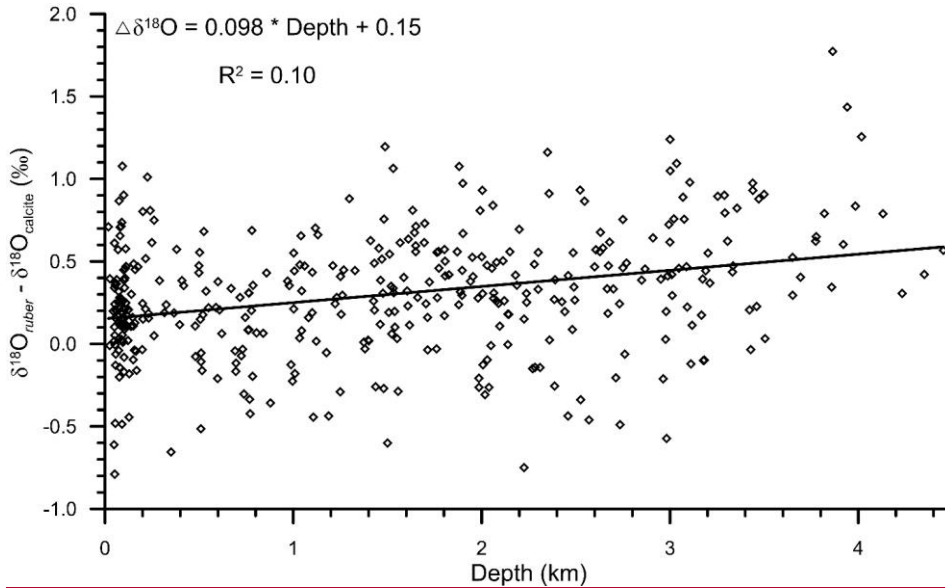
343 We found a strong diagenetic overprinting of $\delta^{18}\text{O}_{ruber}$ in the northern Indian Ocean (Figure 45). The enrichment of
344 $\delta^{18}\text{O}_{ruber}$ with increasing water depth suggests either dissolution leading to the preferential removal of chambers with
345 higher fraction of the lighter oxygen isotope (Wycech et al., 2018), or secondary calcification under comparatively
346 colder water (Lohmann, 1995; Schrag et al., 1995). The increase in planktic foraminifera $\delta^{18}\text{O}$ with increasing depth
347 is a common diagenetic alteration throughout the world oceans (Bonneau et al., 1980). Interestingly, the extent of the
348 increase in $\delta^{18}\text{O}_{ruber}$ with depth in the northern Indian Ocean is much smaller (0.18‰ per thousand meters) than that
349 reported for the same species from the Pacific Ocean (0.4‰ per thousand meters) (Bonneau et al., 1980). However,
350 the increase in $\delta^{18}\text{O}_{ruber}$ with depth in the northern Indian Ocean is continuous, unlike the abrupt shift in $\delta^{18}\text{O}$ (0.3-
351 0.4‰, between the depths above and below the lysocline) of another surface dwelling planktic species, namely
352 *Trilobatus sacculifer*, as observed in the western equatorial Pacific (Wu and Berger, 1989). The smaller increase in
353 $\delta^{18}\text{O}_{ruber}$ with depth is attributed to the shallower habitat of *G. ruber* as compared to *T. sacculifer*. The chamber
354 formation at different water depths implies increased heterogeneity in the *T. sacculifer* shells, with those formed at
355 warmer surface temperature being more susceptible to dissolution as compared to those formed at deeper depths during
356 the gametogenesis phase (Wycech et al., 2018). The chambers in *G. ruber* are formed at a similar depth and therefore,
357 the increase in $\delta^{18}\text{O}_{ruber}$ is continuous, while those of *T. sacculifer* are precipitated at different depths and therefore the
358 shift in $\delta^{18}\text{O}$ after a particular depth. The increase in $\delta^{18}\text{O}_{ruber}$ with depth is mainly due to the partial dissolution of the
359 more porous and thinner parts of the shells secreted at warmer temperature, as such parts are comparatively more
360 susceptible to dissolution (Berger, 1971). The increase in $\delta^{18}\text{O}_{ruber}$ with depth is similar in both the Arabian Sea and
361 BoB.

362 Additionally, the gradual decrease in the sedimentation rate with increasing depth and distance from the
363 continental margins can also cause a depth related trend in $\delta^{18}\text{O}_{ruber}$. The bioturbation disturbs the top few cm
364 sediments (Gerino et al., 1998) resulting in the mixing of older shells with comparatively younger shells (L6wemark,
365 and Grootes, 2004). In high sedimentation rate regions of the shelf and slope, the mixing is restricted to the shells
366 deposited in a shorter, climatologically stable interval. However, in the deeper regions, it is likely that the shells
367 deposited during the colder glacial interval or deglaciation with relatively higher $\delta^{18}\text{O}_{ruber}$ gets mixed with the younger
368 shells, as it is available close to the surface due to the low sedimentation rate (Broecker, 1986; Anderson, 2001). The
369 mixing of shells with a relatively higher $\delta^{18}\text{O}$ with the modern shells having lighter $\delta^{18}\text{O}$ can also result in the depth
370 related increasing trend of $\delta^{18}\text{O}_{ruber}$. The sedimentation rate is very high on the slope and decreases in the deeper
371 regions of both the Arabian Sea (Singh et al., 2017) and BoB (e.g. Bhonsale and Saraswat, 2012; Suokhrie et al.,
372 2022).

373 The large influence of the terrestrial fresh water influx in the shallower region, as compared to the deeper
374 parts of the northern Indian Ocean, is also likely to contribute to the observed increase in $\delta^{18}\text{O}_{ruber}$ with depth. The
375 fresh water is depleted in heavier oxygen isotope as compared to the seawater (Bhattacharya et al., 1985; Ramesh &
376 Sarin, 1992). Thus, the foraminiferal shells secreted in the shallow waters are likely to be enriched in the lighter
377 oxygen isotope, resulting in a depth related bias. Therefore, to delineate the influence of depth related diagenetic

Formatted: Font color: Custom Color(RGB(0,51,204))

378 alteration and secondary calcification in $\delta^{18}\text{O}_{ruber}$, we subtracted the expected $\delta^{18}\text{O}_{calcite}$ from the measured $\delta^{18}\text{O}_{ruber}$.
379 The difference between the measured $\delta^{18}\text{O}_{ruber}$ and expected $\delta^{18}\text{O}_{calcite}$ was plotted with water depth (Figure 12). The
380 difference (measured $\delta^{18}\text{O}_{ruber}$ - expected $\delta^{18}\text{O}_{calcite}$) increased with depth, suggesting a strong influence of the depth
381 related processes in $\delta^{18}\text{O}_{ruber}$.



382
383 **Figure 12: The relationship of the difference between measured $\delta^{18}\text{O}_{ruber}$ and expected $\delta^{18}\text{O}_{calcite}$ with the water depth from**
384 **which the surface samples were collected, in the northern Indian Ocean. The $\delta^{18}\text{O}_{ruber} - \delta^{18}\text{O}_{calcite}$ increased with increasing**
385 **water depth.**
386

387 6.4 Salinity contribution to $\delta^{18}\text{O}_{ruber}$

388 We report a strong influence of salinity on $\delta^{18}\text{O}_{ruber}$ ($R^2=0.63$). As expected, $\delta^{18}\text{O}_{ruber}$ has a direct positive relationship
389 with the ambient salinity. The $\delta^{18}\text{O}_{ruber}$ increased by 0.29‰ for every psu increase in salinity. The northern Indian
390 Ocean has a large salinity gradient (~10 psu) from the lowest in the northern BoB to the highest in the northwestern
391 Arabian Sea. The river water and direct precipitation is enriched in the lighter isotope (Kumar et al., 2010; Kathayat
392 et al., 2021). Thus, the increased riverine influx and precipitation contributes isotopically lighter water to the surface
393 ocean (Rai et al., 2021) and decreases the $\delta^{18}\text{O}_{ruber}$. From the surface seawater samples collected during the winter
394 monsoon season (January-February 1994), a $\delta^{18}\text{O}$ -salinity slope of 0.26‰ was deduced for the Arabian Sea and of
395 0.18‰ for the BoB (Delaygue et al., 2001). However, the $\delta^{18}\text{O}$ -salinity slope varies regionally as well as during
396 different seasons (Singh et al., 2010; Achyuthan et al., 2013). The $\delta^{18}\text{O}$ -salinity slope varied from as low as 0.10 for
397 the coastal BoB samples collected during the months of April-May to as high as 0.51 for the samples collected from

398 the western BoB during the peak south-west monsoon season (August-September 1988) (Singh et al., 2010). The large
399 seasonal variation implies limitations of $\delta^{18}\text{O}$ -salinity slope deduced from snapshot surface seawater samples.
400 Additionally, *G. ruber* flux is reported throughout the year (Guptha et al., 1997), suggesting that the fossil population
401 represents annual average conditions (Thirumalai et al., 2014).

402 A different $\delta^{18}\text{O}_{ruber}$ -salinity slope for the Arabian Sea (0.28) and ~~Bay of Bengal~~BoB (0.19) is attributed to
403 the different hydrographic regimes of these two basins. The runoff and precipitation excess in the BoB results in a
404 comparatively lower salinity as compared to the evaporation dominated Arabian Sea. However, it should be noted
405 here that the relationship between $\delta^{18}\text{O}_{ruber}$ and salinity was very robust for all the northern Indian Ocean samples
406 plotted together. Interestingly, the slope of $\delta^{18}\text{O}$ -salinity for the entire northern Indian Ocean samples is much lower
407 than that for the Atlantic Ocean (0.59 for North Atlantic and 0.52 for South Atlantic, Delaygue et al., 2000) despite
408 the large meltwater influx into the north Atlantic. The dissimilar $\delta^{18}\text{O}$ -salinity slope in different basins and also during
409 different seasons in the same basin is mainly attributed to the variation in the end member composition and the relative
410 amount of fresh water (riverine/precipitation/sub-marine ground water discharge) input from various sources during
411 different seasons (Achyuthan et al., 2013; Tiwari et al., 2013). The heavier oxygen isotope depleted precipitation/fresh
412 water influx in the higher latitudes (~-35 ‰) as compared to the tropical areas (~-5 ‰) also results in a higher slope
413 of the $\delta^{18}\text{O}$ -salinity relationship in the North Atlantic Ocean (Rozanski et al., 1993). Additionally, ~~The~~the difference
414 in $\delta^{18}\text{O}$ -salinity slope despite of the huge fresh water input into both the basins is also because a large fraction of the
415 riverine fresh water spreads across the surface of the northern Indian Ocean, while the melt water sinks to deeper
416 depths in the North Atlantic Ocean. A consistent systematic difference has previously been observed between planktic
417 foraminiferal shells collected in plankton tows and surface sediments, with shells from the sediments being
418 comparatively enriched in ^{18}O (Vergnaud-Grazzini, 1976).

419

420 6.5 Temperature control on $\delta^{18}\text{O}_{ruber}$

421 A first order comparison of the uncorrected $\delta^{18}\text{O}_{ruber}$ with ambient temperature of the top 30 m of the water column at
422 respective stations showed 0.32‰ decrease with every 1°C warming. The change in $\delta^{18}\text{O}_{ruber}$ as inferred from the
423 core-top sediments of the northern Indian Ocean is higher than that estimated from the plankton tows (0.22‰ per 1°C
424 change in temperature) (Mullitza et al., 2003). The seawater temperature was amongst the primary factors identified
425 to affect $\delta^{18}\text{O}_{ruber}$ (Emiliani, 1954; Mullitza et al., 2003). The low correlation between $\delta^{18}\text{O}_{ruber}$ and temperature in this
426 dataset is attributed to the limited temperature variability (1°C, 28-29°C) at a majority of the stations. The large salinity
427 difference (~6.5 psu) between stations further obscures any significant correlation between uncorrected $\delta^{18}\text{O}_{ruber}$ and
428 temperature. The temperature influence on $\delta^{18}\text{O}_{ruber}$ was thus assessed by comparing the ambient temperature with the
429 $\delta^{18}\text{O}_{ruber}$ corrected for $\delta^{18}\text{O}_{sw}$ ($\delta^{18}\text{O}_{ruber} - \delta^{18}\text{O}_{sw}$). The pH of the seawater has also been identified as a factor affecting
430 the stable oxygen isotopic composition of planktic foraminifera (Bijma et al., 1999). However, as argued by Mullitza
431 et al., (2003), the limited modern surface seawater pH variability (Chakraborty et al., 2021) and its close dependence
432 on temperature implies that the pH contribution to $\delta^{18}\text{O}_{ruber}$ is well within the error associated with the measurements.

Formatted: Font color: Custom Color(RGB(0,51,204))

433 The seawater pH in the immediate vicinity of the foraminiferal shell is strongly influenced by the light intensity in the
434 presence of symbionts (Jorgensen et al., 1985). The riverine influx in the northern Indian Ocean makes the surface
435 waters turbid reducing the light penetration depths (Prasanna Kumar et al., 2010). Therefore, riverine influx induced
436 variations in turbidity in the northern Indian Ocean can influence the $\delta^{18}\text{O}_{ruber}$ via the pH effect.

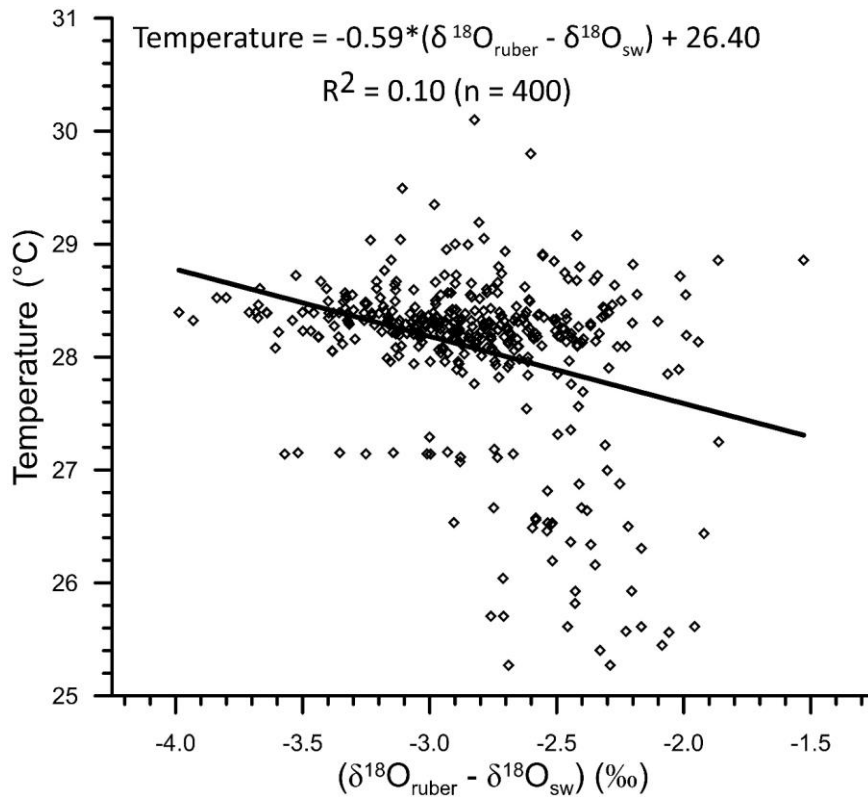
437 The comparison of $\delta^{18}\text{O}_{sw}$ corrected $\delta^{18}\text{O}_{ruber}$ with the ambient temperature also confirms the enrichment of
438 ($\delta^{18}\text{O}_{ruber} - \delta^{18}\text{O}_{sw}$) in heavier oxygen isotope with the decrease in temperature (Figure 4013). We obtained the
439 following relationship between temperature and ($\delta^{18}\text{O}_{ruber} - \delta^{18}\text{O}_{sw}$) in the northern Indian Ocean.

440

441
$$\text{Temperature} = -0.59 * (\delta^{18}\text{O}_{ruber} - \delta^{18}\text{O}_{sw}) + 26.40$$

442

443 The slope of the temperature and ($\delta^{18}\text{O}_{ruber} - \delta^{18}\text{O}_{sw}$) was somewhat different (0.17‰ per 1°C change in temperature)
444 than that of the temperature versus uncorrected $\delta^{18}\text{O}_{ruber}$, but similar as that reported for the plankton tows (0.22‰ per
445 1°C change in temperature) (Mulitza et al., 2003).



446
447

Formatted: Font color: Custom Color(RGB(0,51,204))

Formatted: Font color: Custom Color(RGB(0,51,204))

448 **Figure 4013:** The relationship between ambient temperature and ($\delta^{18}\text{O}_{ruber} - \delta^{18}\text{O}_{sw}$) for the northern Indian Ocean. As
449 expected the ($\delta^{18}\text{O}_{ruber} - \delta^{18}\text{O}_{sw}$) gets enriched in heavier isotope with decreasing ambient temperature.

450

451 7. Conclusions

452 We measured the stable oxygen isotopic ratio of the surface dwelling planktic foraminifera *Globigerooides ruber*
453 white variety from the surface sediments of the northern Indian Ocean. A comparison of the $\delta^{18}\text{O}_{ruber}$ with the depth
454 suggests a strong diagenetic alteration of the isotopic ratio. The ambient salinity exerts the maximum influence on the
455 $\delta^{18}\text{O}_{ruber}$ suggesting its robust application to reconstruct past salinity in the northern Indian Ocean. The large east-west
456 salinity gradient in the northern Indian Ocean results in a strong longitudinal variation in $\delta^{18}\text{O}_{ruber}$. The temperature
457 influence on $\delta^{18}\text{O}_{ruber}$ is subdued as compared to the effect of large salinity variation in the northern Indian Ocean. We
458 report a relatively smaller change in $\delta^{18}\text{O}_{ruber}$ with a unit increase in ambient temperature in case of specimens retrieved
459 from the surface sediments as compared to those collected live from the water column.

460 8. Data Availability

461 The newly generated data as well as the data compiled from previous studies from the northern Indian Ocean has been
462 submitted to PANGAEA and is available at
463 <https://www.pangaea.de/tok/59190adf9e4facf7ebb9ad555c0bce58a9a72bd9> (Saraswat et al., 2022). The data is
464 submitted with the manuscript as well, for the reviewers' scrutiny.

465 9. Author Contribution

466 RS designed the research, compiled and interpreted the data and wrote the manuscript. TS, DKN, DPS, SMS, MS,
467 GS, SRB, SRK picked the specimens for isotopic analysis. MM, ASM supervised the analysis. All authors edited and
468 contributed to the final manuscript.

469 10. Competing Interests

470 The authors declare that they have no conflict of interest.

471 Acknowledgements

472 We thank the crew onboard expeditions during which the surface sediment samples were collected. The authors thank
473 the Director, CSIR-National Institute of Oceanography for the facilities and funding. The technical personnel at the

Formatted: Font color: Custom Color(0,51,204)

Formatted: Font color: Custom Color(0,51,204)

474 Alfred-Wegner Institute for Polar and Marine Research, and MARUM, Bremen University, Germany are
475 acknowledged for the help in stable isotopic analysis. We thank Dr. V. Ramaswamy, CSIR-NIO for providing the
476 surface sediment samples collected from the Myanmar continental shelf. The authors also thank Dr. B.N. Nath for
477 providing the spade core-top samples from the eastern margin of India. We thank Dr. Alberto Sanchez, Centro
478 Interdisciplinario de Ciencias Marinas, Instituto Politécnico Nacional, La Paz, B.C.S, Mexico, and the anonymous
479 reviewer, for their constructive comments and suggestions that helped to improve the manuscript.

480

481

482 **References**

- 483
- 484 Achyuthan, H., Deshpande, R.D., Rao, M.S., Kumar, B., Nallathambi, T., Shashi Kumar, K., Ramesh, R.,
485 Ramachandran, P., Maurya, A.S., and Gupta, S.K.: Stable isotopes and salinity in the surface waters of the Bay of
486 Bengal: Implications for water dynamics and palaeoclimate. *Mar. Chem.*, 149, 51-62, 2013.
- 487 [Anderson, D.M.: Attenuation of millennial-scale events by bioturbation in marine sediments. *Paleoceanography*, 16,](#)
488 [352–357, 2001.](#)
- 489 Bé, A.W.H., and Hutson, W.H.: Ecology of planktonic foraminifera and biogeographic patterns of life and fossil
490 assemblages in the Indian Ocean. *Micropaleontology*, 23, 369, 1977.
- 491 Bemis, B.E., Spero, H.J., Bijma, J., and Lea, D.W.: Reevaluation of the oxygen isotopic composition of planktonic
492 foraminifera: Experimental results and revised paleotemperature equations. *Paleoceanography* 13, 150-160, 1998.
- 493 Berger, W.H.: Sedimentation of planktonic foraminifera. *Mar. Geol.*, 11, 325-358, 1971.
- 494 Berger, W.H., and Killingley, J.S.: Glacial-Holocene transition in deep-sea carbonates: selective dissolution and the
495 stable isotope signal. *Science*, 197, 563-566, 1977.
- 496 Bhadra, S.R., and Saraswat, R.: Assessing the effect of riverine discharge on planktic foraminifera: A case study from
497 the marginal marine regions of the western Bay of Bengal. *Deep Sea Res. II: Topical Stud. Oceanogra.*, 183,
498 104927, 2021.
- 499 [Bhattacharya, S.K., Gupta, S.K. and Krishnamurthy, R.V.: Oxygen and hydrogen isotopic ratios in ground waters and](#)
500 [river waters from India. *Proc. Indian Acad. Sci. \(Earth Planet. Sci.\)*, 94, 283-295, 1985.](#)
- 501 [Bhonsale, S., and Saraswat, R.: Abundance and size variation of *Globorotalia menardii* in the northeastern Indian](#)
502 [Ocean during the late Quaternary. *J. Geol. Soc. India*, 80, 771-782, 2012.](#)
- 503 Bijma, J., Spero, H.J., and Lea, D.W.: Reassessing foraminiferal stable isotope geochemistry: Impact of the oceanic
504 carbonate system (experimental results). In: Fischer, G., Wefer, G. (Eds.), *Use of Proxies in Paleoclimatology:*
505 *Examples from the South Atlantic.* Springer, Berlin, pp. 489-512, 1999.
- 506 Bonneau, M.-C., Vergnaud-Grazzini, C., and Berger, W.H.: Stable isotope fractionation and differential dissolution
507 in Recent planktonic foraminifera from Pacific box-cores. *Oceanologica Acta*, 3, 377-382, 1980.
- 508 Boyer, T. P., Antonov, J. I., Baranova, O. K., Garcia, H. E., Johnson, D. R., Mishonov, A. V., et al.: *World Ocean*
509 *Database*, 2013.
- 510 Bristow, L.A., Callbeck, C.M., Larsen, M., Altabet, M.A., Dekaezemacker, J., Forth, M., Gauns, M., Glud, R.N.,
511 Kuypers, M.M.M., Lavik, G., Milucka, J., Naqvi, S.W. A., Pratihary, A., Revsbech, N. P., Thamdrup, B., Treusch,
512 A.H., and Canfield, D. E.: N₂ production rates limited by nitrite availability in the Bay of Bengal oxygen minimum
513 zone. *Nat. Geosci.*, 10, 24-29, 2017.
- 514 [Broecker, W.S.: Oxygen isotope constraints on surface ocean temperatures. *Quat. Res.*, 26, 121–134,](#)
515 [https://doi.org/10.1016/0033-5894\(86\)90087-6](https://doi.org/10.1016/0033-5894(86)90087-6), 1986.
- 516 Chaitanya, A.V.S., Lengaigne, M., Vialard, J., Gopalakrishna, V.V., Durand, F., Kranthikumar, C., Amritash, S.,
517 Suneel, V., Papa, F., and Ravichandran, M.: Salinity measurements collected by fishermen reveal a “river in the
518 sea” flowing along the eastern coast of India. *Bull. American Met. Soc.*, 95, 1897-1908, 2014.

519 Chakraborty, K., Valsala, V., Bhattacharya, T., and Ghosh, J.: Seasonal cycle of surface ocean pCO₂ and pH in the
520 northern Indian Ocean and their controlling factors. *Progr. Oceanogra.*, 198, 102683, 2021.

521 Chatterjee, A., Kumar, B.P., Prakash, S., and Singh, P.: Annihilation of the Somali upwelling system during summer
522 monsoon. *Sci. Rep.*, 9, 1-14, 2019.

523 Dämmer, L.K., de Nooijer, L., van Sebille, E., Haak, J.G., and Reichert, G.-J.: Evaluation of oxygen isotopes and
524 trace elements in planktonic foraminifera from the Mediterranean Sea as recorders of seawater oxygen isotopes
525 and salinity. *Clim. Past*, 16, 2401-2414, 2020.

526 De Deckker, P.: The Indo-Pacific Warm Pool: critical to world oceanography and world climate. *Geosci. Lett.*, 3, 20,
527 2016.

528 Delaygue, G., Bard, E., Rollion, C., Jouzel, J., Stievenard, M., and Duplessy, J.-C.: Oxygen isotope/salinity
529 relationship in the northern Indian Ocean. *J. Geophys. Res.*, 106, 4565-4574, 2001.

530 Delaygue, G., J. Jouzel, and Dutay, J.C.: Oxygen 18–salinity relationship simulated by an oceanic general circulation
531 model. *Earth Planet. Sci. Lett.*, 178, 113-123, 2000.

532 Duplessy, J.C., Bé, A.W.H., and Blanc, P.L.: Oxygen and carbon isotopic composition and biogeographic distribution
533 of planktonic foraminifera in the Indian Ocean. *Palaeogeogra., Palaeoclimatol., Palaeoecol.*, 33, 9-46, 1981.

534 Duplessy, J.C.: Glacial to interglacial contrasts in the northern Indian Ocean. *Nature*, 295, 494-498, 1982.

535 Duplessy, J.C., Blanc, P.L., and Bé, A.W.H.: Oxygen-18 enrichment of planktonic foraminifera due to gametogenic
536 calcification below the euphotic zone. *Science*, 213, 1247-1250, 1981.

537 Emiliani, C.: Depth habitat of some species of pelagic foraminifera as indicated by oxygen isotope ratio. *American J.*
538 *Sci.*, 252, 149-158, 1954.

539 Erez, J., and Luz, B.: Experimental paleotemperature equation for planktonic foraminifera. *Geochim. Cosmochim.*
540 *Acta*, 47, 1025-1031, 1983.

541 Fairbanks, R. G. and Wiebe, P. H.: Foraminifera and chlorophyll maximum: vertical distribution, seasonal succession,
542 and paleoceanographic significance. *Science (New York, N.Y.)*, 209, 1524–1526,
543 <https://doi.org/10.1126/science.209.4464.1524>, 1980.

544 Fraile, I., Schulz, M., Mülitz, S., and Kucera, M.: Predicting the global distribution of planktonic foraminifera using
545 a dynamic ecosystem model. *Biogeosciences*, 5, 891-911, 2008.

546 Ganssen, G., and Kroon, D.: Evidence for Red Sea surface water circulation from oxygen isotopes of modern surface
547 waters and planktonic foraminiferal tests. *Paleoceanography*, 6, 73-82, 1991.

548 Gerino, M., Aller, R.C., Lee, C., Cochran, J.K., Aller, J.Y., Green, M.A. and Hirschberg, D.: Comparison of different
549 tracers and methods used to quantify bioturbation during a spring bloom: 234-Thorium, luminophores and
550 chlorophyll a. *Estuarine Coast. Shelf Sci.*, 46, 531–547, 1998.

551 ▲

552 Guptha, M.V.S., Curry, W.B., Ittekkot, V., and Muralinath, A.S.: Seasonal variation in the flux of planktic
553 foraminifera: Sediment trap results from the Bay of Bengal, northern Indian Ocean. *J. Foraminiferal Res.*, 27, 5-
554 19, 1997.

Formatted: Font color: Custom Color(RGB(0,51,204))

555 Hemleben, C., Spindler, M., and Anderson, O. R.: Modern Planktonic Foraminifera, Springer-Verlag, New York,
556 1989.

557 Hollstein, M., Mohtadi, M., Rosenthal, Y., Moffa Sanchez, P., Oppo, D., Martínez Méndez, G., Steinke, S., and
558 Hebbeln, D.: Stable oxygen isotopes and Mg/Ca in planktic foraminifera from modern surface sediments of the
559 Western Pacific Warm Pool: Implications for thermocline reconstructions. *Paleoceanography*, 32, 1174-1194,
560 2017.

561 Horikawa, K., Kodaira, T., Zhang, J., and Murayama, M.: $\delta^{18}\text{O}_{\text{sw}}$ estimate for *Globigerinoides ruber* from core-top
562 sediments in the East China Sea. *Progr. Earth Planet. Sci.*, 2, 19, 2015.

563 Howden, S. D., and Murtugudde, R.: Effects of river inputs into the Bay of Bengal. *J. Geophys. Res.*, 106(C9), 19825-
564 19844, 2001.

565 Hut, G.: Consultants group meeting on stable isotope reference samples for geochemical and hydrological
566 investigations. Report to the Director General, International Atomic Energy Agency, Vienna, 42 pp, 1987.

567 [Jørgensen, B. B., Erez, J., Revsbech, P., and Cohen, Y.: Symbiotic photosynthesis in a planktonic foraminiferan,
568 *Globigerinoides sacculifer* \(Brady\), studied with microelectrodes. *Limnol. Oceanogr.*, 30, 1253–1267, 1985.](#)

569 Joseph, S., and Freeland, H.J.: Salinity variability in the Arabian Sea. [Geophysical-Geophys. Research-Res.
570 Letters](#), 32, L09607, 2005.

571 [Kallel, N., Paterne, M., Duplessy, J., Vergnaudgrazzini, C., Pujol, C., Labeyrie, L., Arnold, M., Fontugne, M., and
572 Pierre, C.: Enhanced rainfall in the Mediterranean region during the last Sapropel Event. *Oceanologica Acta*, 20,
573 1997.](#)

574 Kathayat, G., Sinha, A., Tanoue, M., K. Yoshimura, H. Li, Zhang, H., and Cheng, H.: Interannual oxygen isotope
575 variability in Indian summer monsoon precipitation reflects changes in moisture sources. [Communication-Comm.](#)
576 *Earth Environ.*, 2, 96, 2021.

577 Kemle-von-Mücke, S., and Hemleben, C.: Planktic Foraminifera. In: Boltovskoy E (ed) South Atlantic zooplankton.
578 Backhuys Publishers, Leiden, pp 43-67, 1999.

579 Kessarkar, P.M., Purnachandra Rao, V., Naqvi, S.W.A., and Karapurkar, S.G.: Variation in the Indian summer monsoon
580 intensity during the Bölling-Ållerød and Holocene. *Paleoceanography*, 28, 413-425, 2013.

581 Kim, S.T., and O'Neil, J.R.: Equilibrium and nonequilibrium oxygen isotope effects in synthetic carbonates.
582 [Geochimica-Geochim.](#) *Cosmochim. Acta*, 61, 3461-3475, 1997.

583 Kroon, D., and Ganssen, G.: Northern Indian Ocean upwelling cells and the stable isotope composition of living
584 planktonic foraminifers. *Deep-Sea Res.*, 36, 1219-1236, 1989.

585 Kumar, B., S. P. Rai, U. Saravana Kumar, S. K. Verma, P. Garg, S. V. Vijaya Kumar, R. Jaiswal, B. K. Purendra, S.
586 R. Kumar, and N.G. Pande: Isotopic characteristics of Indian precipitation. *Water Resource Res.*, 46, W12548,
587 2010.

588 Lambeck, K., H. Rouby, A. Purcell, Y. Sun, and M. Sambridge: Sea level and global ice volumes from the Last Glacial
589 Maximum to the Holocene. *Proc. Nat. Acad. Sci.*, 111, 15296–15303, 2014.

590 Lea, D.W.: Elemental and isotopic proxies of past ocean temperatures. *Treatise Geochem.*, 8, 373-397, 2014.

591 [Locarnini, R. A., Mishonov, A. V., Baranova, O. K., Boyer, T. P., Zweng, M. M., Garcia, H. E., Reagan, J. R., Seidov,](#)
592 [D., Weathers, K., Paver, C. R. and Smolyar, I.: World Ocean Atlas 2018, Volume 1: Temperature. A. Mishonov](#)
593 [Technical Ed.: NOAA Atlas NESDIS 81, 52pp, 2018.](#)

594 Lohmann, G. P.: A model for variation in the chemistry of planktonic foraminifera due to secondary calcification and
595 selective dissolution. *Paleoceanography*, 10, 445-457, 1995.

596 [Löwemark, L., and Grootes, P.M.: Large age differences between planktic foraminifers caused by abundance](#)
597 [variations and Zoophycos bioturbation. *Paleoceanography*, 19, PA2001, doi:10.1029/2003PA000949, 2004.](#)

598 [Löwemark, L., Hong, W.-L., Yui, T.-F., and Hung, G.-W.: A test of different factors influencing the isotopic signal](#)
599 [of planktonic foraminifera in surface sediments from the northern South China Sea. *Mar. Micropaleontol.* 55, 49-](#)
600 [62, 2005.](#)

601 [Madhu, N.V., Jyothibabu, R., Maheswaran, P.A., Gerson, V.J., Gopalakrishnan, T.C., and Nair, K.K.C.: Lack of](#)
602 [seasonality in phytoplankton standing stock \(chlorophyll a\) and production in the western Bay of Bengal. *Cont.*](#)
603 [Shelf Res.](#), 26, 1868-1883, 2006.

604 Madhupratap, M., S.P. Kumar, P.M.A. Bhattathiri, M.D. Kumar, S. Raghukumar, K.K.C. Nair, and N. Ramaiah:
605 Mechanism of the biological response to winter cooling in the northeastern Arabian Sea. *Nature*, 384, 549-552,
606 1996.

607 Mahesh, B.S., and Banakar, V.K.: Change in the intensity of low-salinity water inflow from the Bay of Bengal into
608 the Eastern Arabian Sea from the Last Glacial Maximum to the Holocene: Implications for monsoon variations.
609 *Palaeogeogra., Palaeoclimatol., Palaeoecol.*, 397, 31-37, 2014.

610 McCorkle, D. C., Martin, P. A., Lea, D. W., and Klinkhammer, G.P.: Evidence of a dissolution effect on benthic
611 foraminiferal shell chemistry: $\delta^{13}\text{C}$, Cd/Ca, Ba/Ca, and Sr/Ca results from the Ontong Java Plateau.
612 *Paleoceanography*, 10, 699-714, 1997.

613 Metcalfe, B., Feldmeijer, W., and Ganssen, G.M.: Oxygen isotope variability of planktonic foraminifera provide clues
614 to past upper ocean seasonal variability. *Paleoceanogra. Paleoclimatol.*, 34, 374–393, 2019.

615 Mohtadi, M., Oppo, D.W., Lückge, A., DePol-Holz, R., Steinke, S., Groeneveld, J., Hemme, N., and Hebbeln, D.:
616 Reconstructing the thermal structure of the upper ocean: Insights from planktic foraminifera shell chemistry and
617 alkenones in modern sediments of the tropical eastern Indian Ocean. *Paleoceanography*, 26, PA3219, 2011.

618 Mulitza, S., Boltovskoy, D., Donner, B., Meggers, H., Paul, A., and Wefer, G.: Temperature: $\delta^{18}\text{O}$ relationships of
619 planktonic foraminifera collected from surface waters. *Palaeogeogra., Palaeoclimatol., Palaeoecol.*, 202, 143-152,
620 2003.

621 Mulitza, S., Dürkoop, A., Hale, W., Wefer, G., and Niebler, H.S.: Planktonic foraminifera as recorders of past surface-
622 water stratification. *Geology*, 25, 335-338, 1997.

623 Mulitza, S., Wolff, T., Pätzold, J., Hale, W., and Wefer, G.: Temperature sensitivity of planktic foraminifera and its
624 influence on the oxygen isotope record. *Mar. Micropaleontol.*, 33, 223-240, 1998.

625 Naqvi, S.W.A.: Deoxygenation in marginal seas of the Indian Ocean. *Front. Mar. Sci.*, 8, 624322. doi:
626 10.3389/fmars.2021.624322, 2021.

627 Naqvi, S.W.A., H. Naik, A. Pratihary, W. D'souza, P.V. Narvekar, D.A. Jayakumar, A.H. Devol, T. Yoshinari, and T.
628 Saino: Coastal versus open-ocean denitrification in the Arabian Sea. *Biogeosciences*, 3, 621-633, 2006.

629 Panchang, R., and Nigam, R.: High resolution climatic records of the past~ 489 years from Central Asia as derived
630 from benthic foraminiferal species, *Asterorotalia trispinosa*. *Mar. Geol.*, 307, 88-104, 2012.

631 Pearson, P.N.: Oxygen isotopes in foraminifera: Overview and historical review. In *Reconstructing Earth's Deep-*
632 *Time Climate—The State of the Art in 2012*, Paleontological Society Short Course, November 3, 2012. The
633 Paleontological Society Papers, Volume 18, Linda C. Ivany and Brian T. Huber (eds.), pp. 1-38, 2012.

634 Prasanna Kumar, S., J. Narvekar, M. Nuncio, M. Gauns, and S. Sardesai: What drives the biological productivity of
635 the northern Indian Ocean? Washington DC American Geophysical Union Geophysical Monograph Series, 185,
636 33-56, 2009.

637 [Prasanna Kumar, S., Narvekar, J., Nuncio, M., Kumar, A., Ramaiah, N., Sardesai, S., Gauns, M., Fernandes, V., and](#)
638 [Paul J.: Is the biological productivity in the Bay of Bengal light limited? *Curr. Sci.*, 98, 1331-1339, 2010.](#)

639

640 Prasanna Kumar, S., M. Nuncio, J. Narvekar, A. Kumar, D.S. Sardesai, S.N. De Souza, M. Gauns, N. Ramaiah, and
641 M. Madhupratap: Are eddies nature's trigger to enhance biological productivity in the Bay of Bengal? *Geophys.*
642 *Res. Lett.*, 31, L07309, doi:10.1029/2003GL019274, 2004.

643 Prasanna Kumar, S., and Prasad, T.G.: Formation and spreading of Arabian Sea high-salinity water mass. *J. Geophys.*
644 *Res: Oceans*, 104, 1455-1464, 1999.

645 Prell, W.L., and Curry, W.B.: Faunal and isotopic indices of monsoonal upwelling: Western Arabian Sea.
646 *Oceanologica Acta*, 4, 91-98, 1981.

647 Qasim, S.Z.: Biological productivity of the Indian Ocean. *Indian J. Mar. Sci.*, 6, 122-137, 1977.

648 Rai, S.P., J. Noble, D. Singh, Y.S. Rawat, and B. Kumar: Spatiotemporal variability in stable isotopes of the Ganga
649 River and factors affecting their distributions. *Catena*, 204, 105360, 2021.

650 Ramaswamy, V., Gaye, B., Shirodkar, P.V., Rao, P.S., Chivas, A. R., Wheeler, D., and Thwin, S.: Distribution and
651 sources of organic carbon, nitrogen and their isotopic signatures in sediments from the Ayeyarwady (Irrawaddy)
652 continental shelf, northern Andaman Sea. *Mar. Chem.*, 111, 137-150, 2008.

653 [Ramesh, R. and Sarin, M.M.: Stable isotope study of the Ganga \(Ganges\) river system. *J. Hydrology*, 139, 49-62,](#)
654 [1992.](#)

655 Rao, R. R., and Sivakumar, R.: Seasonal variability of sea surface salinity and salt budget of the mixed layer of the
656 north Indian Ocean. *J. Geophys. Res.*, 108(C1), 3009, 2003.

657 Rixen, T., ~~G. Cowie~~, ~~G. B. Gaye~~, ~~B. J. Goes~~, ~~J. H. do Rosário Gomes~~, ~~H. R. R. Hood~~, ~~R. R. Z. Lachkar~~, ~~Z. H.~~
658 ~~Schmidt~~, ~~H. J. Segsneider~~, ~~J.~~ and ~~A. Singh~~, ~~A.~~: Reviews and syntheses: Present, past, and future of the oxygen
659 minimum zone in the northern Indian Ocean. *Biogeosciences*, 17, 6051-6080, 2020.

660 Rochford, D. J.: Salinity maximum in the upper 100 meters of the north Indian Ocean. *Aust. J. Mar. Freshwater Res.*,
661 15, 1-24, 1964.

662 [Rozanski, K., Araguás-Araguás, L., and Gonfiantini, R.: Isotopic Patterns in Modern Global Precipitation, in: Climate](#)
663 [Change in Continental Isotopic Records, edited by: Swart, P. K., Lohmann, K. C., Mckenzie, J., and Savin, S.,](#)
664 [American Geophysical Union, Washington, D. C., 1–36, <https://doi.org/10.1029/GM078p0001>, 1993.](#)

665 Saalim, S.M., Saraswat, R., and Nigam, R.: Ecological preferences of living benthic foraminifera from the Mahanadi
666 river-dominated north-western Bay of Bengal: A potential environmental impact assessment tool. *Mar. Poll. Bull.*,
667 175, 113158, 2022.

668 [Sánchez, A., Sánchez-Vargas, L., Balart, E., and Domínguez-Samalea, Y.: Stable oxygen isotopes in planktonic](#)
669 [foraminifera from surface sediments in the California Current system. *Mar. Micropaleontol.*, 173, 102127, 2022.](#)

670 Saraswat, R., Lea, D.W., Nigam, R., Mackensen, A., and Naik, D.K.: Deglaciation in the tropical Indian Ocean driven
671 by interplay between the regional monsoon and global teleconnections. *Earth Planet. Sci. Lett.*, 375, 166-175,
672 2013.

673 Saraswat, R., Nigam, R., Mackensen, A., and Weldeab, S.: Linkage between seasonal insolation gradient in the tropical
674 northern hemisphere and the sea surface salinity of the equatorial Indian Ocean during the last glacial period. *Acta*
675 *Geol. Sinica*, 86, 801–811, 2012.

676 Saraswat, R., ~~D.P.~~ Singh, ~~D.P.~~, ~~D.W.~~ Lea, ~~D.W.~~, ~~A.~~ Mackensen, ~~A.~~ and ~~D.K.~~ Naik, ~~D.K.~~: Indonesian throughflow
677 controlled the westward extent of the Indo-Pacific Warm Pool during glacial-interglacial intervals. *Global Planet.*
678 *Cha.*, 183, 103031, 2019.

679 Saraswat, R., Suokhrie, T., Naik, D.K., Singh, D.P., Saalim, S.M., Salman, M., Kumar, G., Bhadra, S.R., Mohtadi,
680 M., Kurtarkar, S.R., and Maurya, A.S., ~~2022~~: Oxygen isotopic ratio of *Globigerinoides ruber* (white variety) in
681 the surface sediments of the northern Indian Ocean. PANGAEA, <https://doi.org/10.1594/PANGAEA.945401>,
682 ~~2022~~.

683 [Sarma, V.V. and Aswanikumar, V.: Subsurface chlorophyll maxima in the north-western Bay of Bengal. *J. Plankton*](#)
684 [Res., 11, 339-352, 1991.](#)

685 Sarma, V.V.S.S., M-Chopra, ~~M.~~, ~~D.N.~~ Rao, ~~D.N.~~, ~~M.M.R.~~ Priya, ~~M.M.R.~~, ~~G.R.~~ Rajula, ~~G.R.~~, ~~D.S.R.~~ Lakshmi, ~~D.S.R.~~,
686 and ~~V.D.~~ Rao, ~~V.D.~~: Role of eddies on controlling total and size-fractionated primary production in the Bay of
687 Bengal. *Cont. Shelf Res.*, 204, 104186, 2020.

688 [Schlitzer, R., Ocean Data View, <https://odv.awi.de>, 2018.](#)

689 Schmidt, G.A., Bigg, G.—R., and Rohling, E.J.: "Global Seawater Oxygen-18 Database - v1.22"
690 <https://data.giss.nasa.gov/o18data/>, 1999.

691 [Schmidt, M.W., Spero, H.J., and Lea, D.W.: Links between salinity variation in the Caribbean and North Atlantic](#)
692 [thermohaline circulation. *Nature*, 428, 160–163, 2004.](#)

693 Schrag, D.P., DePaolo, D.J., Richter, F.M.: Reconstructing past sea surface temperatures: Correcting for diagenesis
694 of bulk marine carbonate. *Geochim. Cosmochim. Acta*, 59, 2265–2278, 1995.

695 Sengupta, D., Bharath Raj, G.N., and Shenoi, S.S.C.: Surface freshwater from Bay of Bengal runoff and Indonesian
696 Throughflow in the tropical Indian Ocean. *Geophys. Res. Lett.*, 33, L22609, 2006.

697 Shackleton, N.J.: Oxygen isotopes, ice volume and sea level. *Quat. Sci. Rev.*, 6, 183-190, 1987.

698 Shackleton, N.J.: The 100,000-year Ice-Age cycle identified and found to lag temperature, carbon dioxide, and orbital
699 eccentricity. *Science*, 289, 1897-1902, 2000.

700 Shackleton, N.J., and Vincent, E.: Oxygen and carbon isotope studies in recent foraminifera from the southwest Indian
701 ocean. *Mar. Micropaleontol.*, 3, 1-13, 1978.

702 Shankar, D., Vinayachandran, P.N., and Unnikrishnan, A.S.: The monsoon currents in the north Indian Ocean. *Progr.*
703 *Oceanogra.*, 52, 63–120, 2002.

704 Shetye, S.R., Gouveia, A.D., and Shenoi, S.S.C.: Circulation and water masses of the Arabian Sea. *Proc. Indian Acad.*
705 *Sci. (Earth Planet. Sci.)*, 103, 107-123, 1994.

706 Shetye, S.R., ~~S.S.C.~~ Shenoi, ~~S.S.C., A.D.~~ Gouveia, ~~A.D., G.S.~~ Michael, ~~G.S., D.~~ Sundar, ~~D.~~, and ~~G.~~ Nampoothiri, ~~G.~~:
707 Wind-driven coastal upwelling along the western boundary of the Bay of Bengal during the southwest monsoon.
708 *Cont. Shelf Res.*, 11, 1397-1408, 1991.

709 Singh, A., Jani, R.A., and Ramesh, R.: Spatiotemporal variations of the $\delta^{18}\text{O}$ –salinity relation in the northern Indian
710 Ocean. *Deep-Sea Res. I*, 57, 1422–1431, 2010.

711 [Singh, D.P., Saraswat, R., and Naik, D.K.: Does glacial-interglacial transition affect sediment accumulation in](#)
712 [monsoon dominated regions? *Acta Geol. Sinica*, 91, 1079-1094, 2017.](#)

713 Singh, D.P., Saraswat, R., and Nigam, R.: Untangling the effect of organic matter and dissolved oxygen on living
714 benthic foraminifera in the southeastern Arabian Sea. *Mar. Poll. Bull.*, 172, 112883, 2021.

715 Sirocko, F.: Zur Akkumulation von Staubsedimenten im nördlichen Indischen Ozean; Anzeiger der Klimageschichte
716 Arabiens und Indiens. Dissertation, Berichte-Reports, Geologisch-Paläontologisches Institut der Universität Kiel,
717 27, 185 pp, 1989.

718 Smitha, A., ~~K.A.~~ Joseph, ~~K.A., C.~~ Jayaram, ~~C.~~, and ~~A.N.~~ Balchand, ~~A.N.~~: Upwelling in the southeastern Arabian Sea
719 as evidenced by Ekman mass transport using wind observations from OCEANSAT–II Scatterometer. *Indian J.*
720 *Geo-mar. Sci.*, 43, 111-116, 2014.

721 Spero, H.J., Bijma, J., Lea, D.W., and Bemis, B.B.: Effect of seawater carbonate concentration on foraminiferal carbon
722 and oxygen isotopes. *Nature*, 390, 497-500, 1997.

723 Sridevi, B., and ~~V.V.S.S.~~ Sarma, ~~V.V.S.S.~~: A revisit to the regulation of oxygen minimum zone in the Bay of Bengal.
724 *J. Earth Syst. Sci.*, 129, 1-7, 2020.

725 Stainbank, S., Kroon, D., Rüggeberg, A., Raddatz, J., de Leau, E.S., Zhang, M., et al.: Controls on planktonic
726 foraminifera apparent calcification depths for the northern equatorial Indian Ocean. *PLoS ONE* 14(9), e0222299,
727 2019.

728 Suokhrie, T., Saraswat, R., and Nigam, R.: Multiple ecological parameters affect living benthic foraminifera in the
729 river-influenced west-central Bay of Bengal. *Front. Mar. Sci.*, 8, 467, 2021a.

730 Suokhrie, T., Saraswat, and R., Saju, S.: Strong solar influence on multi-decadal periodic productivity changes in the
731 central-western Bay of Bengal. *Quat. Int.*, <https://doi.org/10.1016/j.quaint.2021.04.015>, 2021b.

732 Thirumalai, K., Richey, J.N., Quinn, T.M., and Poore, R.Z.: *Globigerinoides ruber* morphotypes in the Gulf of
733 Mexico: A test of null hypothesis. *Sci. Rep.*, 4, 6018, 2014.

734 Thompson, P.R., Bé, A.W.H., Duplessy, J.-C., and Shackleton, N.J.: Disappearance of pink-pigmented
735 *Globigerinoides ruber* at 120,000 yr BP in the Indian and Pacific oceans. *Nature*, 280, 554-558, 1979.

736 [Thunell, R., Tappa, E., Pride, C., and Kincaid, E.: Sea-surface temperature anomalies associated with the 1997–1998](#)
737 [El Niño recorded in the oxygen isotope composition of planktonic foraminifera. *Geology*, 27, 843.](#)
738 [Waelbroeck, C., Mulitza, S., Spero, H., Dokken, T., Kiefer, T., and Cortijo, E.: A global compilation of late Holocene](https://doi.org/10.1130/0091-7613(1999)027<0843:SSTAAW>2.3.CO;2, 1999.</p><p>739 Tiwari, M., Nagoji, S.S., Kartik, T., Drishya, G., Parvathy, R.K., and Rajan, S.: Oxygen isotope–salinity relationships
740 of discrete oceanic regions from India to Antarctica vis-à-vis surface hydrological processes. <i>J. Mar. Syst.</i>, 113–
741 114, 88-93, 2013.</p><p>742 Urey, H.-C.: The thermodynamic properties of isotopic substances. <i>J. Chem. Soc.</i>, 12, 562-569, 1947.</p><p>743 Vergnaud-Grazzini, C.: Non-equilibrium isotopic compositions of shells of planktonic foraminifera in the
744 Mediterranean Sea. <i>Palaeogeogra., Palaeoclimatol., Palaeoecol.</i>, 20, 263-276, 1976.</p><p>745 Vinayachandran, P.N., and Shetye, S.R.: The warm pool in the Indian Ocean. <i>Proc. Indian Acad. Sci. (Earth Planet</i>
746 <i>Sci.)</i> 100, 165-175, 1991.</p><p>747 <a href=)
748 [planktonic foraminiferal \$\delta^{18}\text{O}\$: relationship between surface water temperature and \$\delta^{18}\text{O}\$. *Quat. Sci. Rev.*, 24, 853–](#)
749 [Wang, L., Sarnthein, M., Duplessy, J.-C., Erlenkeuser, H., Jung, S., and Pflaumann, U.: Paleo sea surface salinities in](https://doi.org/10.1016/j.quascirev.2003.10.014, 2005.</p><p>750 <a href=)
751 [the low-latitude Atlantic: The \$\delta^{18}\text{O}\$ record of *Globigerinoides ruber* \(white\). *Paleoceanography*, 10, 749-761, 1995.](#)

752 Wu, G., and Berger, W.H.: Planktonic foraminifera: differential dissolution and the quaternary stable isotope record
753 in the west equatorial Pacific. *Paleoceanography*, 4, 181-198, 1989.

754 Wycech, J.B., Kelly, D.C., Kitajima, K., Kozdon, R., Orland, I.J., and Valley, J.W.: Combined effects of gametogenic
755 calcification and dissolution on $\delta^{18}\text{O}$ measurements of the planktic foraminifer *Trilobatus sacculifer*. *Geochem.*
756 *Geophys. Geosys.*, 19, [Zweng, M.M., Reagan, J.R., Seidov, D., Boyer, T.P., Locarnini, R.A., Garcia, H.E., Mishonov, A.V., Baranova,](https://doi.org/10.1029/2018GC007908, 2018.</p><p>757 <a href=)
758 [O.K., Weathers, K., Paver, C.R. and Smolyar, I.: World Ocean Atlas 2018, Volume 2: Salinity. A. Mishonov](#)
759 [Technical Ed.: NOAA Atlas NESDIS 82, 50pp, 2018.](#)